Chemical Geology 529 (2019) 119280

Contents lists available at ScienceDirect

Chemical Geology

journal homepage: www.elsevier.com/locate/chemgeo

Springwater provenance and flowpath evaluation in Blue Lake, Bonneville basin, Utah

Jory Chapin Lerback[a,*], Scott A. Hynek[a,b], Brenda B. Bowen[a,c], Christopher D. Bradbury[a], D. Kip Solomon[a], Diego P. Fernandez[a]

[a] Department of Geology & Geophysics, University of Utah, Frederick Albert Sutton Building, 115 S 1460 E, Room 383, Salt Lake City, UT 84112-0102, USA
[b] U.S. Geological Survey - Utah Water Science Center, 2329 West Orton Circle, West Valley City, UT 84119-2047, USA
[c] Global Change and Sustainability Center, University of Utah, Frederick Albert Sutton Building, 115 S 1460 E, Room 234, Salt Lake City, UT 84112-0102, USA

ARTICLE INFO

Editor: Karen Johannesson

Keywords:
Groundwater
Isotope chemistry
Bonneville basin
Geochemistry

ABSTRACT

Water in Utah and Nevada is important for agriculture, municipal use, solute transport, and ecosystem preservation. Large spring wetland systems occur on the playa margin of the Bonneville basin, including Blue Lake, 15 km south of the Bonneville Salt Flats on the Utah-Nevada state border. Large spring systems have historically been studied as water budgets don't apparently balance from direct mountain front recharge (Nelson and Mayo, 2014; Gardner and Heilweil, 2014; and others). Blue Lake is no exception; prior studies here have suggested discharge rates 0.04 - 0.05 km^3/yr (Louderback and Rhode, 2009), greater than expected for modelled recharge in the surrounding mountain range (0.03 km^3/yr). Three hypothesized recharge mechanisms for Blue Lake are tested: mountain-front recharge, interbasinal groundwater flow, and infiltration from historic Lake Bonneville. Remote sensing suggests that a conservative estimate of Blue Lake discharge constitutes 50-64% of modelled mountain-front recharge (Flint et al., 2011). Major ions, $\delta^{18}O$, $\delta^{2}H$, dissolved gases (^{14}C, ^{3}He, ^{4}He, Ne, Ar, Kr, Xe) and trace elements (Sr and $^{87}Sr/^{86}Sr$ isotopes) comprehensively constrain recharge conditions, water-rock interactions, flowpaths, and groundwater provenance of this large spring system. ^{14}C signatures suggest that Blue Lake discharge has a transit time between 5,600 and 12,200 years, older than that of Fish Springs. Noble gas concentrations in Blue Lake water suggest an elevated recharge temperature greater than 19°C and low salinity, indicating a deep water table and high geothermal gradient in the recharge area. $^{87}Sr/^{86}Sr$ ratios of playa-margin springs are elevated from that of mid-playa groundwaters, springwaters from the adjacent mountain range, and alluvial fill groundwater from the valley directly south of Blue Lake. Playa-margin spring Sr isotope values (0.713-0.714) are most similar to direct runoff from the Deep Creek Range granodiorite outcrop (> 0.713). Interbasinal groundwater flow in combination with mountain-front recharge is best supported by chemical data rather than mountain-front recharge alone or the slow discharge of regional aquifers recharged by lacustrine infiltration from Lake Bonneville.

1. Introduction

Groundwater flow in the western United States is important for human use and ecosystem function. Understanding subsurface water movement directions and rates, and the related chemical evolution of the water can help clarify water rights across geopolitical boundaries, planning for agricultural, industrial, and municipal groundwater use, subsurface storage, and for understanding the solute flux. In the closed Bonneville basin in Utah's West Desert (traditionally Newe/Western Shoshone and Goshute lands), this solute flux is linked to landscape evolution and the deposition of saline resources that are harvested throughout the Great Salt Lake Desert. Preserving the biodiversity of aridland springs is inherently valuable. Additionally, the wetland deposits associated with these springs are important for preserving paleoenvironmental changes through the Holocene and Pleistocene (Davis et al., 2017; Louderback and Rhode, 2009; Stevens and Meretsky, 2008; Unmack and Minckley, 2008).

Large, mesothermal springs such as Fish Springs in Utah, springs in Ash Meadows in Nevada, and the Furnace Creek springs in California have been studied as part of the Great Basin Carbonate and Alluvial Aquifer System (defined by Heilweil and Brooks, 2010). These springs and associated aquifers have been studied due to concerns of water

* Corresponding author.
E-mail addresses: jory.lerback@utah.edu (J.C. Lerback), shynek@usgs.gov (S.A. Hynek), brenda.bowen@utah.edu (B.B. Bowen), christopher.bradbury@utah.edu (C.D. Bradbury), kip.solomon@utah.edu (D.K. Solomon), diego.fernandez@utah.edu (D.P. Fernandez).

https://doi.org/10.1016/j.chemgeo.2019.119280
Received 11 April 2019; Received in revised form 7 August 2019; Accepted 14 August 2019
Available online 31 August 2019

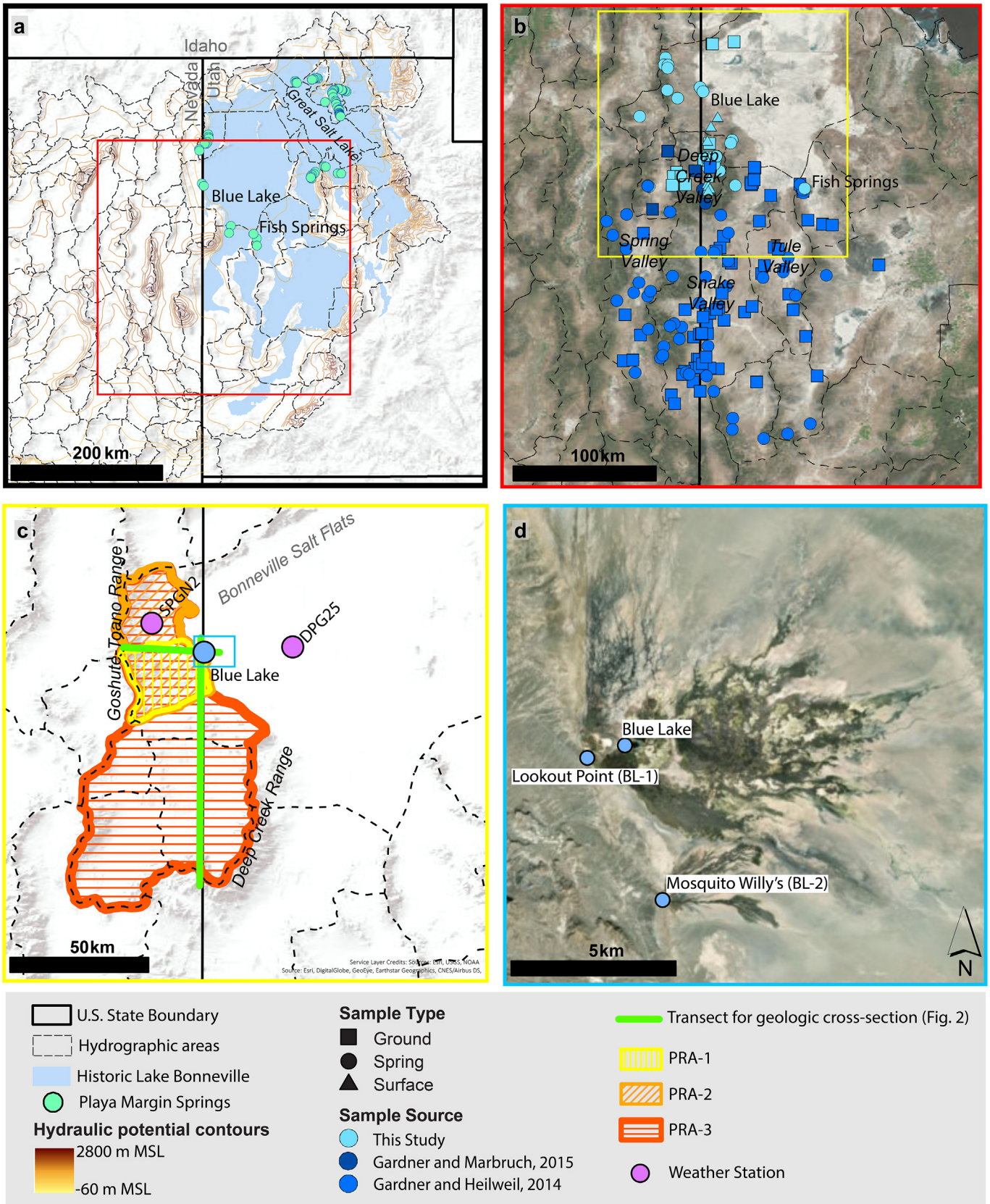

Fig. 1. Field area maps. a) Regional map of the Bonneville basin with location of playa-margin springs. Hydraulic potential contours from the GBCAAS model included (Heilweil and Brooks, 2010); b) map of spring, groundwater, and surface water sample sites used in this study, including this study, water chemistry data from Gardner and Heilweil (2014) to the south, and samples in the Deep Creek Valley published by Gardner and Masbruch (2015); c) map of Proposed Recharge Areas (PRA's), weather station locations (SPGN2 and DPG25), and transect locations for subsurface cross sections, PRA1 represents the most conservative recharge area, the direct topographic watershed of Blue Lake. PRA2 represents the recharge potential for the entire Goshute-Toano Range as a watershed leading to Blue Lake. PRA3 represents both the Goshute-Toano Range and the Deep Creek Range and Valley as a recharge source; d) aerial image of the Blue Lake wetlands with the following sampling points marked: Lookout Point, Blue Lake, and Mosquito Willy's.

rights and connectivity across state borders, and in the case of Ash Meadows and Furnace Springs because of concerns of groundwater contamination from Yucca Mountain's proposed nuclear waste storage site. However, the water budgets of these springs are not well constrained. It is further speculated that discharge at these springs cannot be supported by modern recharge on proximal mountain fronts (Nelson and Mayo, 2014; Gardner and Heilweil, 2014; Gillespie et al., 2012; Bushman et al., 2010; Belcher et al., 2009; Anderson et al., 2006; Winograd, 1962; Harrill and Prudic, 1998; and others). Such springs dot the perimeter of the Bonneville basin in the northeastern extent of the Great Basin region, yet the provenance and flowpaths supporting the discharge at these springs are not well constrained (Fig. 1A).

Blue Lake is part of a series or springs and associated wetlands, with perennial discharge of 28 °C brackish waters on the Utah-Nevada border (Fig. 1). Louderback and Rhode (2009) suggested a discharge rate at Blue Lake of 1.3–1.6 cms (~0.05 km^3/yr) in the Blue Lake ponds, which is much greater than the recharge expected for the entire adjacent valley, with greater elevations and potential recharge, the Deep Creek Valley (16,000 acre-ft/yr or ~0.02 km^3/yr), just southwest of Blue Lake (Gardner and Masbruch, 2015). Additionally, Blue Lake provides useful insights into the current inputs of solutes and groundwater into the Bonneville Salt Flat system, ~15 km to the north. Recent changes in this landscape have instigated investigation into the processes driving changes in the salt system, of interest for mining, mitigation, and recreational purposes (Bowen et al., 2018; Bowen et al., 2017). In Nevada, groundwater is used for agriculture and supports spring and creek systems managed by the Bureau of Land Management. Many springs in the Great Basin have recently dried due to falling groundwater table elevations associated with groundwater extraction (Heilweil and Brooks, 2010; Waddell et al., 1987). Constraining the groundwater provenance and flowpaths at Blue Lake presents an opportunity to test hypotheses about mountain front versus intra-basinal groundwater flow, to evaluate the history of fluid-rock interactions that have resulted in the unique saline resources of this basin, and to define the connectedness or isolation of aquifers.

1.1. Study area

Blue Lake discharges at the western edge of the Bonneville basin. The Bonneville basin is a closed basin at 1300 m elevation that is a geomorphic remnant of Pleistocene Lake Bonneville (Oviatt et al., 2015). The basin occupies the eastern edge of the Great Basin, which is characterized by north-south trending mountain ranges bound by extensional faults (Heilweil and Brooks, 2010; Harrill and Prudic, 1998). To the west of Blue Lake is the Goshute-Toano range, which has highly faulted limestone and dolostone outcrops and a Miocene rhyolite volcanic unit (Fig. 2). Both Blue Lake and Fish Springs discharge to the Bonneville Basin playa at an elevation of 1296 and 1314 m, respectively. The Bonneville basin is characterized by a very flat topography, filled with calcareous lacustrine sediments from Late Pleistocene and Holocene paleolakes, including Lake Bonneville. Isolated lenses of evaporites cap the lacustrine sediments in some areas (Bowen et al., 2018; Oviatt et al., 2015; Turk et al., 1973). Just south of Blue Lake is the Deep Creek Range and the Deep Creek Valley, which is filled with similar alluvial and lacustrine sediments, and is intruded by a Late Eocene/Early Miocene andesite volcanic unit in the Deep Creek Valley (Gardner and Masbruch, 2015; Sweetkind et al., 2011; Coats, 1987; Moore and Sorensen, 1979; Hose and Blake Jr, 1970). The Deep Creek Range is comprised of limestone and dolomite, with a granodiorite intrusion Late Eocene to early Miocene in age (Fig. 2). Research on the geothermal energy potential of this area mapped gravity gradients and interpreted basinal faults in the region between Blue Lake and the closest recharge sites, consistent with those expected from Basin and Range extension (Blackett et al., 2013; Smith et al., 2011; Heilweil and Brooks, 2010; Cook et al., 1964) and the structural histories (Gans et al., 1985). Deep faults and the thin crust associated with the extensional terrane were proposed as the conduit for heat transfer to the groundwater system. Wells near the Bonneville Salt Flats reflect calculated geothermal gradients of 40–70 °C/km, similar to expected geothermal gradient for the Basin and Range Province (Smith et al., 2011; Coolbaugh et al., 2005). Groundwater would not need to circulate > 150 to 250 m deep to gain the 10 °C elevated temperatures seen at the mesothermal springs in this study.

The Blue Lake wetland was cored to reconstruct paleoenvironments from pollen records, from ~15 ka to near present (Louderback and Rhode, 2009). This showed a record of increasing aridity, with a cool, wet period during the Younger Dryas, consistent with other paleoenvironmental reconstructions in Great Basin region. A deeper section of this core extends to 10–45 ka and $\delta^{18}O$, $\delta^{13}C$, and paleomagnetic proxies suggest lake oscillations (Benson et al., 2011). The sedimentary record at Blue Lake suggests that this region generally transitioned from a wet and cool climate in the Late Pleistocene and Early Holocene, to a hot and dry climate, with the exception of an episode of regional cooling at 8 ka (Louderback and Rhode, 2009). The chemical composition of ecological materials reliant on water and springs around the Bonneville basin has also been studied in the context of human occupation and includes a rich archaeological record. The Bonneville basin's Old River Bed Inland Delta, Danger Cave, Bonneville Estates Rockshelter and Camels Back Cave are archaeological sites within the study area which have been investigated and materials dated to compare to paleoenvironmental records at Blue Lake that include the last ~15 ka (Schmitt and Lupo, 2018; Goebel et al., 2011; Louderback et al., 2011).

1.2. Hypothesized springwater flowpaths

We test three hypothesized recharge mechanisms contributing to discharge at Blue Lake, possibly involving a combination of these sources.

1.2.1. Hypothesis 1: mountain-front recharge

The simplest hypothesized source of water at Blue Lake is mountain-front recharge from the Goshute-Toano Range to the west of Blue Lake. Water recharged in the carbonate and volcanic unit in the Goshute-Toano Range would show evidence of carbonate weathering from water-rock interactions in the carbonate aquifer, low recharge temperatures, and high recharge elevations. This type of direct mountain-front recharge flowpath is argued to supply water to Furnace Springs in Death Valley by Bushman et al. (2010) and Anderson et al. (2006), making an argument for short and simple flowpaths with transient recharge rates. The modern discharge at these Death Valley springs is predominantly water recharged from wetter climates in the Holocene. Based on aquifer geometry and hydraulic conductivity estimates made using the Great Basin Carbonate and Alluvial Aquifer System (GBCAAS) conceptual model, flowpaths to Blue Lake from the Goshute-Toano Range would average 5.9 ka (σ = 3.5 ka, $n_{flowpath}$ = 266) (Brooks et al., 2014).

1.2.2. Hypothesis 2: interbasinal groundwater flow

Interbasinal groundwater flow suggests large quantities of groundwater flow beneath topographic watershed divides. This idea was originally proposed in the context of fractured carbonate rocks, where fracture dissolution may enhance or sustain high horizontal hydraulic conductivities and therefore move water relatively quickly, over long distances (Winograd, 1962). The concept of interbasinal groundwater flow was subsequently modified to encompass both carbonate and non-carbonate rocks (Davisson et al., 1999), as well as regional flow between alluvial basin aquifers as described by Toth (1963). In the Bonneville basin, gravity-mapped faults coincide with many major springs on the edge of the Bonneville marl (Smith et al., 2011) (Fig. 1). However, the modern faults characteristic of the extensional terrain in the Great Basin may not cut across the carbonate horsts. Additionally, Caine et al. (2002) assert that faults such as these can operate as baffles,

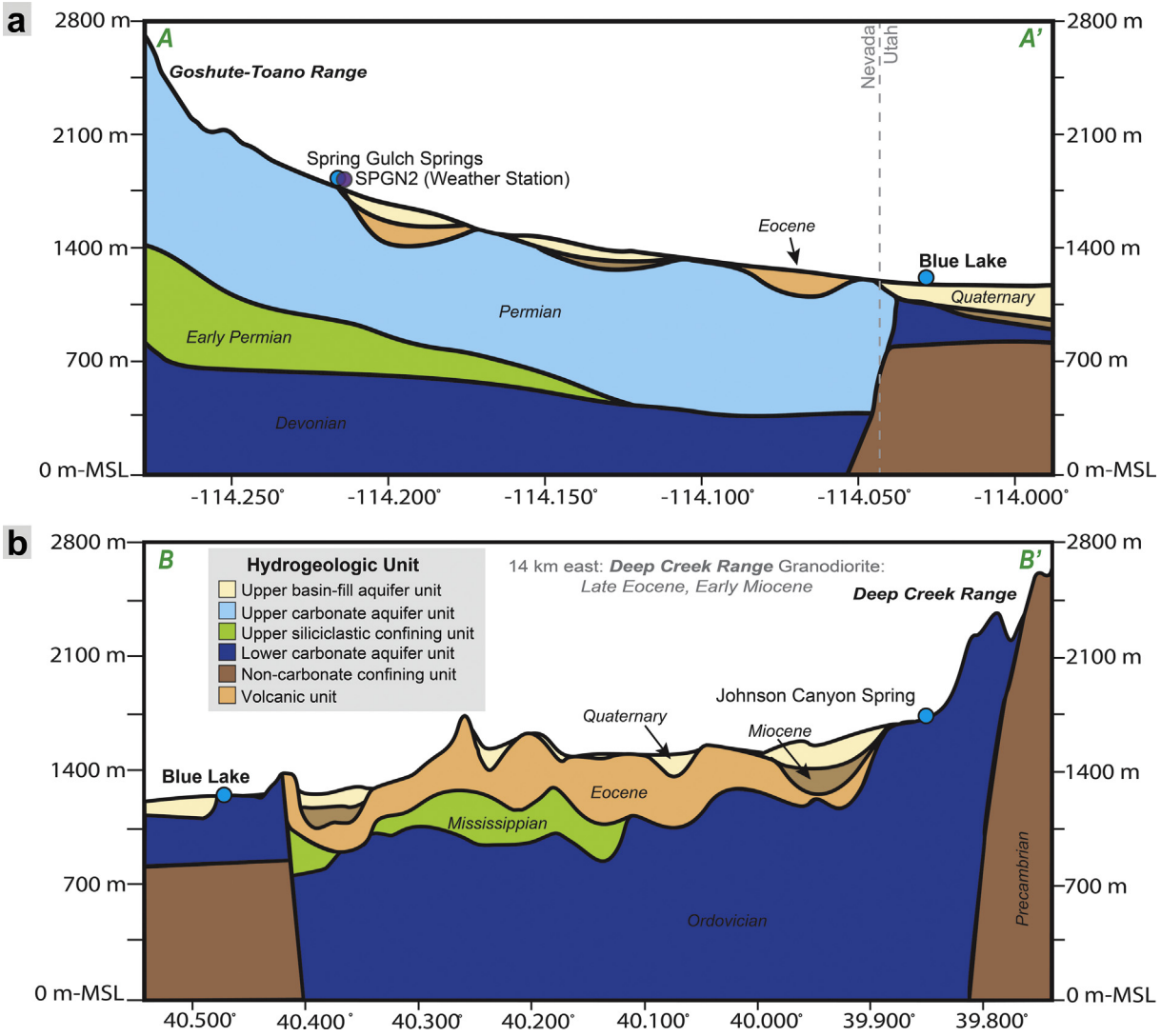

Fig. 2. Schematic cross sections of Blue Lake region. a) West-East conceptual geologic cross section where the Goshute-Toano Range is to the West, and Blue Lake and the Bonneville basin are to the East. c) North-South conceptual geologic cross section showing the Deep Creek Valley to the south in relation to Blue Lake. The highest points of the North-South trending Deep Creek Range are to the East of the displayed cross-section. We estimate the maximum thicknesses of the regional aquifer system based on work by Sweetkind et al. (2011) for the GBCAAS conceptual model. They interpret the depth of a relatively impermeable basement unit called the Non-Carbonate Confining Unit throughout the GBCAAS area. Interpretations in the area of this study show that the Volcanic Unit does not exceed 500 m in thickness within the study area. The lower carbonate aquifer unit is typically 1000–2000 m but are up to 3000 m thick in the study area. There is an upper carbonate unit that, can be up to 2000 m thick. These two layers are sometimes separated by a thin (< 500 m thick) siliciclastic unit. Alluvial basin fill aquifers along the valleys are typically 0–500 m thick but may be up to 1000 m thick in the Deep Creek Valley.

preventing fault-perpendicular flow.

Using interbasinal groundwater flow to balance the steady state water budget at Blue Lake, water from the Deep Creek Valley would be required in addition to Goshute-Toano Range recharge based on a backwards simulation of the GBCAAS model (Brooks et al., 2014). The flowpaths would likely flow through the basin fill alluvial aquifer but may interact with the andesite and rhyolite volcanic units in the northern Deep Creek Valley. The GBCAAS model's aquifer geometry and hydraulic conductivity shows that flowpaths connecting the Goshute-Toano Range to Blue Lake range from 2.4 to 287.4 ka transit times with an average of 11.0 ka (σ = 25.2 ka $n_{flowpath}$ = 294). Flowpaths from the Deep Creek Valley average 59.4 ka (σ = 62.8 ka, $n_{flowpath}$ = 28).

1.2.3. Hypothesis 3: lacustrine infiltration

Infiltration of piedmont aquifers by Lake Bonneville at its higher elevations has been suggested by Oviatt et al. (2015) to explain the formation of organic rich muds observed in sediments of the Great Salt Lake as Lake Bonneville continued its regression from the early Holocene. Freshwater infiltration from the highstand of the lake may have been stored in upslope limestone aquifers and slowly discharged at lower lake shorelines. This would have created a freshwater cap on the increasingly saline Great Salt Lake and led to the observed deposits of alternating salt and sapropel units in the early Holocene. Lacustrine infiltration, if it occurred around the Bonneville basin, would provide water and the hydrologic potential gradient for discharge at other springs around the Bonneville basin. Continuous discharge from these piedmont aquifers may also explain the persistence of wetlands and mesic adapted mammals throughout the Great Basin well into the early Holocene (Schmitt and Lupo, 2018). This mechanism for recharge does not work with the GBCAAS model as it is a steady state solution as described by Brooks et al. (2014) and does not incorporate changes in recharge area or amounts through time.

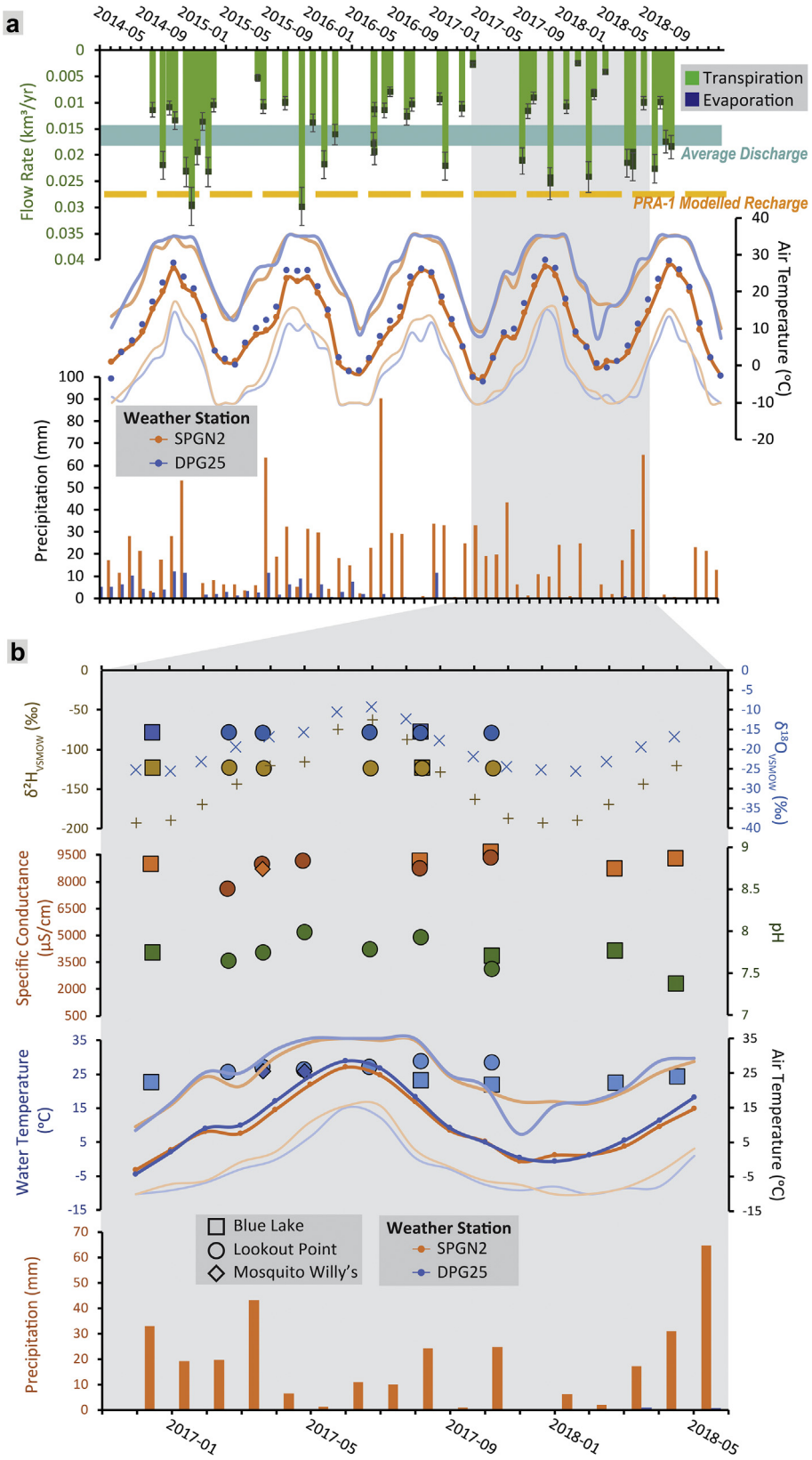

Fig. 3. Temporal changes in constraints on Blue Lake water budget. a) Time series of estimated ET rates, air temperature, and precipitation from NDVI and NDWI landsat image analyses. Error bars on estimated ET rates represent maximum and minimum ET rates for marshland and open water measured by Welch et al. (2007). Estimated recharge for PRA1 noted (Heilweil and Brooks, 2010). b) Bimonthly $\delta^{18}O$ and $\delta^{2}H$ isotope data, specific conductance, pH, water and air temperature, and precipitation from two sampling sites at Blue Lake from 2017 to 2018.

2. Methods

2.1. Field characterization and collection

Water samples were collected throughout the region surrounding Blue Lake ($n = 84$) from fall 2016 to summer 2018 (Fig. 1). These samples were analyzed for a wide range of geochemical parameters to understand the spatial and temporal sources of the groundwater. Samples include existing wells with data generated by the United States Geological Survey (USGS; see Supplementary Data). Groundwater, springs, and surface waters were sampled in the Goshute-Toano Range and the Deep Creek Valley following USGS guidelines (Wilde and Radtke, 1998). Some mid-playa spring samples were collected for trace element analysis and contributed by Bradbury (2019) (see Supplementary Data)A 91 m deep well on the playa edge of the Bonneville Salt Flats and shallow Bonneville Salt Flats brines with depths of 3.7 and 29 m were also sampled (Fig. 1). A YSI® multiparameter probe or a Hydrolab® MS5 multiparameter Mini Sonde was used for in-situ measurements of pH, specific conductance, and water temperature. These data were used to identify the most likely discharge point of larger springs based on spatial gradients in temperature and specific conductivity. Samples were collected from springs and artesian wells under natural free-flowing conditions. Other wells were purged a minimum of one casing volume under low-flow conditions until multi-parameter probe readings parameters stabilized.

2.2. Water budget estimation at Blue Lake

Direct measurement of spring discharge is difficult at Blue Lake, as there are multiple points of direct discharge into the springs, as well as diffuse recharge. Since there is no runoff from Blue Lake, all groundwater must be either evaporated from surface water or transpired by the phreatophytic vegetation. Distal surface water bodies such as the Great Salt Lake or ephemeral standing water at the Bonneville Salt Flats were not considered recharge sources as the regional potentiometric surface from Heilweil and Brooks (2010) does not indicate directional flow between there areas. Therefore, multispectral LANDSAT satellite data was used to quantify the area covered by vegetation to estimate evapotranspiration flux (ET) rates from the area associated with the Blue Lake spring system. Forty-four Landsat scenes from 2014 to 2018 were analyzed using normalized difference water index (NDWI) and the normalized difference vegetation index (NDVI). We manually determined a conservative threshold for both indices to apply to all images in order to quantify the areal footprint and to estimate discharge of the Blue Lake wetland over time (Thomas et al., 2015; Welch et al., 2007). NDVI and NDWI thresholds of −0.160 and − 0.004, respectively, were determined to be a most conservative estimate of vegetation and open water without encompassing the reflectance values of meadowland and grasses associated with rain events, or playa evaporites. ET rates were applied for both wetland and open water areas to estimate the discharge.

2.3. Chemical analyses

Water samples were analyzed for major ion and trace element composition, stable oxygen and hydrogen isotopes, tritium, noble gasses (Xe, Kr, Ar, Ne, He), radiocarbon, sulfur hexafluoride, and strontium isotopes. Chemical analyses followed methods used by the U.S. Geological Survey. Ion chromatography analyses for samples collected with the USGS were performed at the USGS National Water Quality Lab and other samples at Activation Laboratories Ltd. to characterize the major ion and trace element geochemistry. Charge balance was reported within 10%. Laser Water Isotope Analyzer Picarro L2130i was used at the SIRFER laboratory at the University of Utah to measure $\delta^{18}O$ and $\delta^{2}H$ isotopes. Vacuum extraction, mass spectrometry and gas chromatography were used to analyze noble gas, tritium and SF_6 at the Noble Gas Lab at the University of Utah. The National Ocean Sciences Accelerator Mass Spectrometry (NOSAMS) at Woods Hole Oceanographic Institution analyzed all ^{14}C samples. ICP-MS following Mackey and Fernandez (2011) was used to measure trace elements and strontium isotope ratios. Details about the particular methods used for these analyses are reviewed in the appendices.

3. Results

3.1. Climate and landscape change through time

The study area in northwest Utah and northeast Nevada is arid, as is reflected in climate data for areas near Blue Lake obtained through MesoWest, Western Regional Climate Center (WRII), and PRISM (Fig. 1C). Mesowest climate records were obtained from 2007 to 2017 from weather station DPG2 (mid-playa, 25 km east of Blue Lake) and SPGN2 (20 km northwest of Blue Lake in the Goshute-Toano Range). DPG2 records a mean annual temperature of 11.8 °C ($n = 1{,}048{,}563$, $\sigma = 12.08$) (Fig. 3A). The average maximum monthly temperatures are in July at 40.0 °C and minimums are in January at −17.8 °C. DPG2 recorded an average of 297 mm/yr. Weather stations recorded similar precipitation in the Goshute-Toano Range (station SPGN2). WRII data from Ferguson Spring, Ibapah, and Gold Hill show similar results for average temperature and precipitation. PRISM climate models for the 30-year averages (1981–2010) at each of these sites show similar precipitation and temperature ranges, suggesting that the climate of this area has not shifted significantly in the last decades.

The water temperature of Blue Lake varies through the year by 5 °C around a mean of 26 °C (Fig. 3B). Water at Blue Lake has an average specific conductance of 8900 μS/cm and 4.8 per mille salinity. The $\delta^{2}H_{VSMOW}$ and $\delta^{18}O_{VSMOW}$ in the samples from Blue Lake did not vary though seasons. The $\delta^{2}H_{VSMOW}$ varied by 4.6‰ from −123.7‰ ± 0.17 in January 2017 to −125.0‰ ± 0.28 in September 2017. $\delta^{18}O_{VSMOW}$ did not show this difference; the lightest oxygen value was seen in March 2017 of −15.9‰ ± 0.03, and the heaviest in April 2017 with a value of −16.0‰ ± 0.04. The range of hydrogen and oxygen isotopes falls within expected range for meteoric water in this area and plots below the global and modelled local meteoric water line (Craig, 1961). The oxygen and hydrogen isotopes measured through the year compare most closely to modelled precipitation in cooler months.

3.2. Water budget estimation at BL

Previous estimates of groundwater discharge at Blue Lake are 1.3–1.6 cubic meters per second, or 0.04–0.05 km^3/yr (Louderback and Rhode, 2009). However, water discharging to Blue Lake is diffuse throughout the wetland, where the water table is shallow (0–2 m below ground surface). Water at Blue Lake does not move via runoff to anywhere else on the playa and is either directly evaporated from ponds or is transpired by phreatophytic vegetation. Runoff and re-infiltration into the playa sediments is not a persistent feature of the water budget; though event driven recharge may impact the water budget (cf. Boutt et al., 2016). The average area covered by phreatophytic vegetation as estimated from the NDVI analysis is 11.8 km^2 from 2014 to 2018 ($\sigma = 5.44$, $n = 44$). The average area with open water as determined by the NDWI analysis is 0.17 km^2 ($\sigma = 0.30$, n = 44).

We apply a range of expected evaporation rates to the area of open water (1.402–1.707 m/yr) (Welch et al., 2007). To account for the wide variability of ET due to different vegetation types, we use the ET rate minimum of 1.097 m/yr, as the minimum ET for meadowland groundcover (Welch et al., 2007). The ET rate maximum we used was 1.402 m/yr the maximum reported ET rate for marshland groundcover by Welch et al. (2007). The vegetation at Blue Lake is likely a mixture of these vegetation types and “true” ET rate between the rates reported. We applied this range of ET rates to the NDVI determined areas and

added open water evaporation range to estimate the total ET of the Blue Lake wetland for each time period. While the estimated discharge fluctuated through the years, the average calculated volumetric discharge ranges from 0.013 to 0.016 km^3/yr (Fig. 3A).

We compare these discharge estimates to the recharge occurring within three Proposed Recharge Areas based on topographic watershed divides (referred to as PRA1–3, shown in Fig. 1C). Modern mountain-front recharge exemplified by PRA1–2 could supply enough water to Blue Lake, but the conservative discharge estimate here would represent 50–64% of the recharge modelled for PRA1. PRA3 was designed to allow for interbasinal groundwater flow to balance the water budget under current climate conditions, although there are many more areas where runoff, pumping, and ET must be considered, as shown in the water budget estimated for the Deep Creek Valley (Gardner and Masbruch, 2015). Recharge for these PRAs were extracted from the Basin Characterization Model (Flint and Flint, 2007) and adjusted as described by Heilweil and Brooks (2010) for the GBCAAS Model. Heilweil and Brooks (2010) report the pre-development recharge estimates with ± 50% error rate. Thus, this general comparison, which ignores the potential for transience in the complex aquifer system provides preliminary estimates of the water budget. The estimated discharge at Blue Lake is less than the estimated recharge for each PRA1–3 (0.027, 0.053, and 0.269 km^3/yr).

3.3. Groundwater geochemistry

Major ion composition of waters separated into six k-means cluster groups that are associated with the solute loads from mountain front springs, deep basinal groundwaters, and playa-margin sampling locations (Fig. 4A). These data show a wide range of chemical variability in the waters of this area, as has been previously discussed in Gardner and Heilweil (2014). Blue Lake samples are dominantly Na-Cl type waters (Cluster 1) and plot near the waters at the Bonneville Salt Flats on the piper diagram (Fig. 4B). Fish Springs and other playa-margin springs are cluster 3, which are intermediate Na–Cl–SO_4 type waters. Waters nearer the basins and playas are mixed Ca–Mg–SO_4 type (Cluster 2). Cluster 4 represents intermediate waters found in open basins that are trend from Ca–Mg–HCO_3 towards the Ca–Mg–SO_4 Cluster 2 waters. Much of the mountain-front spring and groundwater samples are Ca–Mg–HCO_3 type (Clusters 5, 6), which correlates with the dominance of limestone aquifers (Heilweil and Brooks, 2010). The evolution of major ion chemistry is dominated by the relatively rapid accumulation of solutes by dissolution of evaporite minerals such as gypsum and halite, thus obscuring further interpretations related to groundwater provenance (Gardner and Heilweil, 2014).

Ground- and spring- water in the study area range from −12 to −17‰ $\delta^{18}O$ and −100 to −135‰ $\delta^{2}H$ in a continuous group (Fig. 5). This group plots near the global meteoric water line. Isotopic end-members from these varied recharge sources may be well mixed in the aquifers and/or represent a seasonally averaged groundwater recharge, both of which explain the near-continuous range in isotopic values. Surface water and shallow groundwater samples from the Bonneville Salt Flats playa are outside of this group but follow the expected evolution of evaporative processes.

3.4. Dissolved gasses

The dissolved gasses ^{14}C, ^{3}H, Ne, Ar, Kr, and Xe in groundwater represent compositions of the atmosphere when it was either above ground or in the unsaturated zone. He isotope compositions in water can reflect terrigenic production of gasses within the aquifer and accumulation can in general be correlated with groundwater residence times. SF_6 concentrations can represent either atmospheric conditions or terrigenic production.

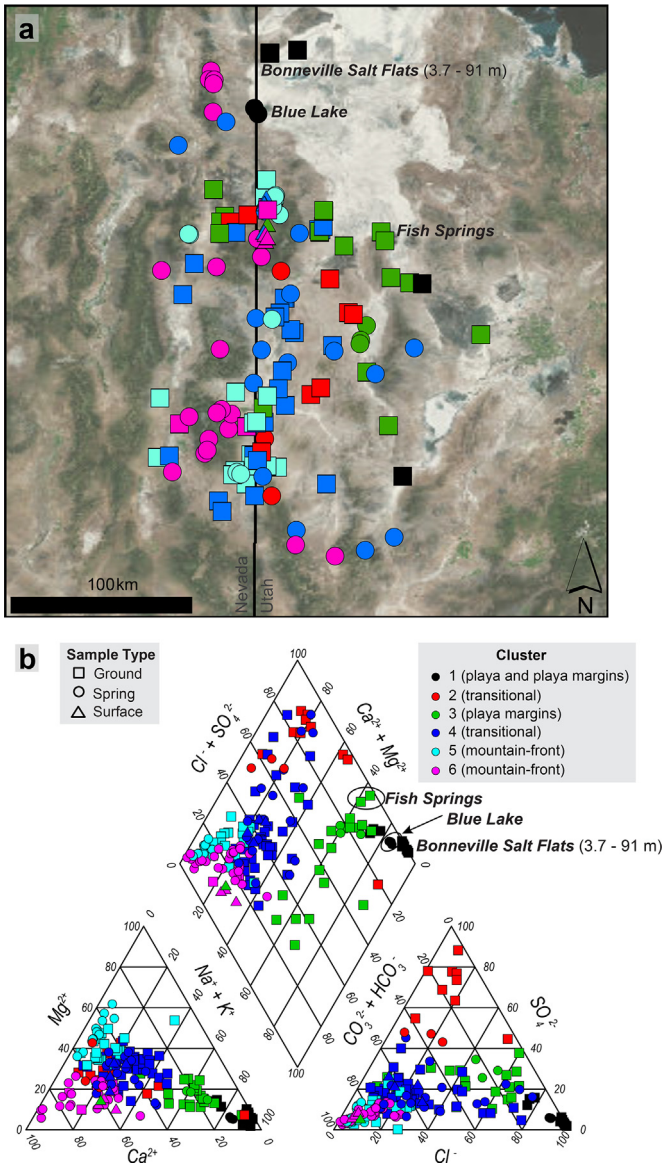

Fig. 4. Major ion chemistry. a) Location of samples with major ions classifications, with shapes and colors by k-means clusters. Statistical analyses of geochemical data were performed in R v3.4. K-means clustering delineate different groups based on the major ion data (Alkalinity as $CaCO_3$, Na^+, K^+, Mg^{+2}, Ca^{+2}, Ba^{+2}, Cl^-, SO_4^{-2}, Br^-). The clustering used scaled data and the Hartigan and Wong (1979) method. Number of clusters was determined using the silhouette index (Rousseeuw, 1987). b) Piper diagram of samples colored by k-means clusters.

3.4.1. Radiocarbon: proxy for mean groundwater transit time

Radiocarbon was used to evaluate the reasonable range of groundwater transit times at the specific sample site. Carbon is not a closed system as it moves from recharge area to location of sampling, thus we employed several complementary methods to understand the reactions taking place in order to reasonably estimate the ranges of groundwater mean transit times. Comparison of ^{14}C, $\delta^{13}C$ and dissolved inorganic carbon (DIC) (after Han and Plummer, 2013) shows that the dominant mechanism of C isotope evolution in playa-margin springs and other groundwaters < 50% of modern carbon (pmC) is the weathering of carbonates (Fig. 6A, Appendix D). Some younger samples, mostly associated with mountain front recharge likely represent mixtures of meteoric water that have not fully undergone carbon-exchange in the soil root zone, which we modelled with a $\delta^{13}C$ of 22‰ in this area (Hart et al., 2010). Using the carbon isotopes from each sample, we applied

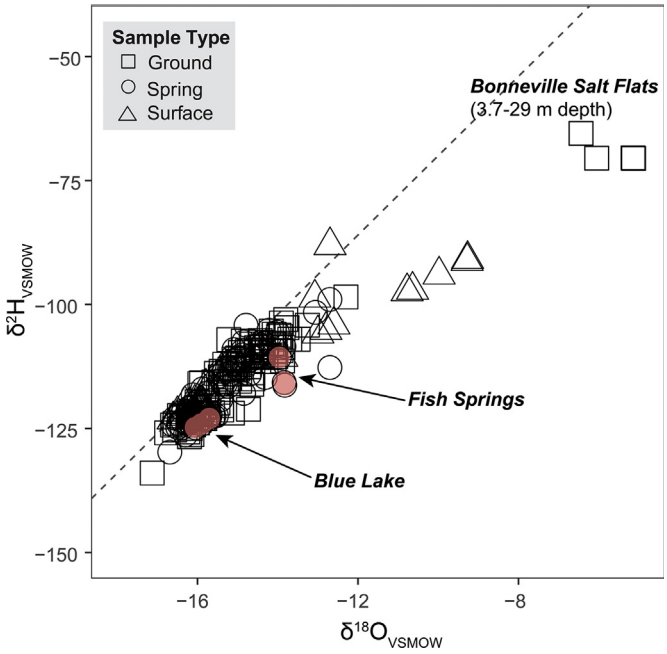

Fig. 5. Stable hydrogen and oxygen isotopes in study region. Samples are shown in comparison to the global meteoric water line (Craig, 1961).

updated Fontes and Garnier (1979) model by Han and Plummer (2016) to model carbonate dissolution and the International Atomic Energy Agency's model (Gonfiantini, 1972) to model the potential mixing of groundwater flowpaths. This combination of models estimates a range of apparent groundwater ages that we interpret as mean transit times as they likely represent mixtures of a spectrum of flow paths. For example, the pmC at Blue Lake's Lookout Point is 8.5 pmC with a standard deviation of 0.07 pmC and Mosquito Willy's, a smaller spring 3.8 km south, with 6.58 pmC and a standard deviation of 0.08 pmC. The Han and Plummer (2013) updated Fontes and Garnier (1979) and IAEA models suggest ages of 5.5–10.8 ka for Blue Lake and 1.7–12.2 ka for Mosquito Willy's. Previous USGS analyses of Mosquito Willy's in 1981 suggest uncorrected ages of 21,600 ka (USGS, 2019), similar to the uncorrected age of 21,859 ka calculated from 6.58 pmC collected in 2017 as reported by NOSAMS. Fish Springs was sampled in three ponds: Persey Spring, Mirror Spring and North Spring, which have radiocarbon transit times of modern-6.3 ka. All data and modelled ages are reported in Supplementary data.

3.4.2. Tritium: proxy for mean groundwater transit time

As each groundwater and spring water sample may be a mixture of converging flowpaths of different lengths and a variety of transit times, tritium was measured to evaluate the proportion of modern recharge in each sample. Mountain-front springs had in excess of 5 TU, indicating a large component of modern recharge (water having equilibrated with the atmosphere after the early 1960's nuclear testing). The radiocarbon in these samples, where measured, had close to 100 pmC. There was no anthropogenic tritium found in the water at most basinal groundwaters and springs, including Lookout Point at Blue Lake (0.03 TU), suggesting a negligible component of water recharged in a post-bomb era.

3.4.3. Sulfur hexafluoride: proxy for mean groundwater transit time

Dissolved SF_6 was collected in addition to tritium to evaluate the component of modern recharge at several springs. However, SF_6 is also known to accumulate in groundwater because of terrigenic production (von Rohden et al., 2010; Deeds et al., 2008; Busenberg and Plummer, 2000). Samples in the Deep Creek Valley showed generally atmospheric values, which are at or below ≤9.4 parts per trillion by volume partial pressure (pptv) or the expected modern local atmospheric

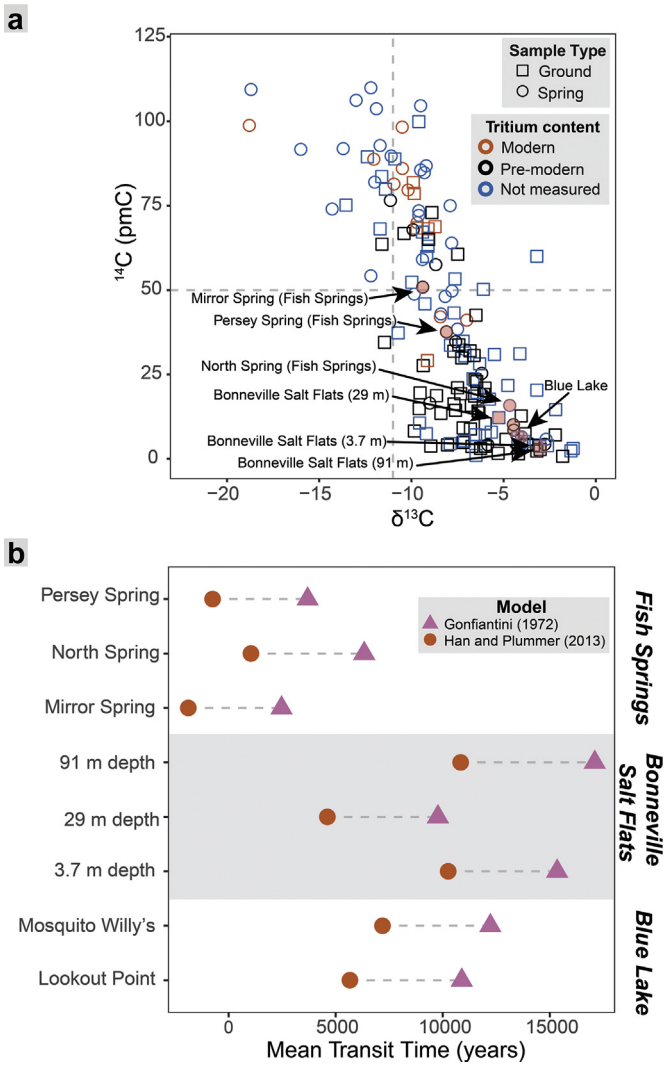

Fig. 6. Carbon isotopic evolution. a) Percent modern radiocarbon activity as related to $\delta^{13}C$ composition of ground and spring water samples. Vertical dashed line represents the modelled 0.5 * -22‰ of expected carbon isotope exchange of plants in the Bonneville basin (Hart et al., 2010). Horizontal dashed line represents 0.5 * modern ^{14}C (50 pmC). b) Modelled mean transit times for select samples using models from Han and Plummer (2013) and Gonfiantini (1972).

concentration (National Oceanic and Atmospheric Administration, 2017), but had some terrigenic component preventing their use as groundwater transit time indicators. Blue Lake, the Bonneville Salt Flats wells at 91 and 29 m depths, and Mud Springs in the Goshute-Toano Range had clearly terrigenic SF_6 levels (> 9.4 pptv) and were thus not used here to interpret short flowpath mixing. More information on these data and sample locations can be found in Appendix G.

3.4.4. Helium: proxy for mean groundwater transit time

Helium isotopes in the Basin and Range have been used as indicators of geothermal activity and can show evidence of mantle degassing (Genereux et al., 2009; Kennedy and van Soest, 2007; Crossey et al., 2006; Graham, 2002; Pinti and Marty, 1998; Solomon et al., 1996). The isotopic composition of $^3He/^4He$ (R) is based on the comparison of $^3He/^4He$ to air which is 1.38×10^{-6}, here (R_a) (Sano et al., 2013; Solomon et al., 1996). The R/R_a in the mantle is 8 or higher due to the presence of ^3He as a primordial nuclide (Stuart et al., 2003; Graham, 2002). Groundwater transit times are generally associated with the accumulation of ^4He from ^{238}U, ^{235}U, and ^{232}Th decay by the

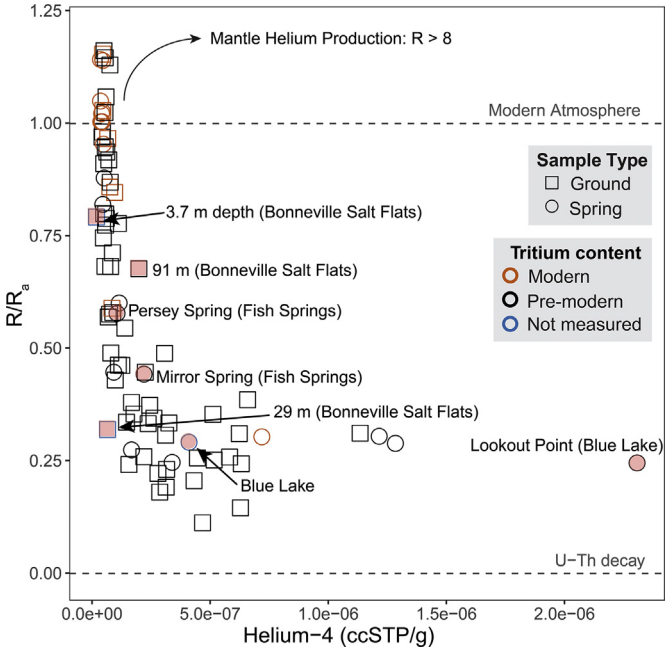

Fig. 7. Helium isotopes. a) Ratio of helium isotopes in water to that in air (R/R_a) versus Helium-4 content.

expulsion of alpha particles into the groundwater (Andrews, 1985; Torgersen and Ivey, 1985). Thus, groundwater R/R_a can evolve asymptotically towards 0.02 with the addition of crustal He, or towards 8+ with the addition of mantle helium which can occur in tectonically active areas (Banerjee et al., 2011; Nelson et al., 2009; Kennedy et al., 1997).

The waters in this study area evolve towards neither of these end-members (Fig. 7). Samples increase in ^{4}He concentration and decrease the R/R_a but evolve towards a R/R_a of 0.26. While this suggests the dominant mechanism for ^{4}He accumulation is U and Th decay, a small component of mantle degassing in structurally deformed areas such as at the fault on the Bonneville basin margin just west of Blue Lake, may account for the 0.26 R value reached at Blue Lake. This has been seen in other areas of the Basin and Range Province associated with geothermal energy potential (Banerjee et al., 2011; Kennedy and van Soest, 2007), and differentiates Blue Lake from Fish Springs and wells on the Bonneville Salt Flats.

Terrigenic helium (He_{terr}) is the fraction of total He-4 that is from crustal or mantle origin. He_{terr} does not include ^{4}He from equilibrium solubility with the atmosphere or excess air and was calculated using (1) neon concentration and (2) derived from a closed-system equilibrium model using Ne, Ar, Kr, and Xe concentrations (Aeschbach-Hertig and Solomon, 2013). Accumulation of He_{terr} in water is thought to be generally related to pmC as accumulation increases with residence times as shown in Fig. A5 (Solomon and Cook, 2000).

3.4.5. Noble gas recharge temperatures

Following the methodology of Gardner and Heilweil (2014) we calculated noble gas recharge temperatures (NGTs) using a closed-system equilibration model solution with acceptable uncertainties ($\Sigma\chi^2 > 6.64$) (Kipfer et al., 2002; Aeschbach-Hertig et al., 2000). NGTs using the midpoint of possible altitudes of the possible recharge (NGT_{avg}) were used so as to have directly comparable model solutions to those reported by Gardner and Heilweil (2014). These samples were modelled with 0 or 0.25‰ salinity for Gardner and Heilweil (2014) and Gardner and Masbruch (2015), respectively. Spatial distribution of NGT_{avg}s are shown in Fig. 8A.

NGT_{avg}s can be used to delineate separations between aquifer recharge zones. NGTs from 11 to 15.4 °C, or modern measured mountain

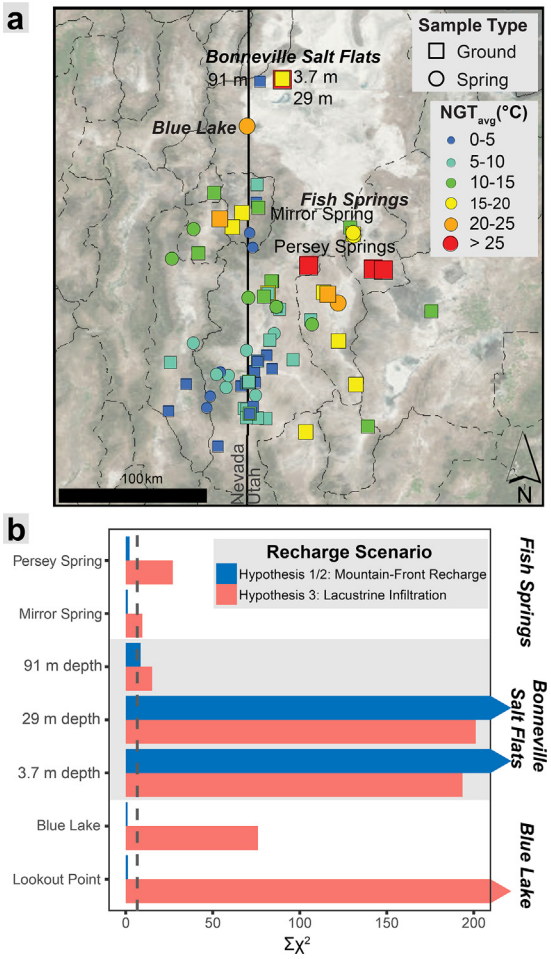

Fig. 8. Noble gasses modelled recharge temperatures and model fits. a) Map of sample locations with associated average noble gas recharge temperatures (after Gardner and Heilweil, 2014). b) Model fits for selected samples with two recharge scenarios representing Hypothesis 1/2 and Hypothesis 3 using a closed-system, unfractionated model with variable temperature and salinity. Model results with $\Sigma\chi^2 \leq 6.64$ are acceptable fits (to the left of the vertical dotted line).

and valley water-table temperatures as used by Gardner and Heilweil (2014), were used to delineate a basinal difference of water source. Spatial divisions within the dataset on NGT_{avg}s expanded from Gardner and Heilweil (2014) in Fig. 8A are also apparent at the 15 °C mark in the Deep Creek Valley, where the deeper groundwater wells display higher NGT_{avg}s, and mountain-front springs have cooler NGT_{avg}s. The Bonneville basin springs have generally higher NGT_{avg}s than the measured water table temperatures and the NGT_{avg}s in Snake and Spring Valleys. We note the difference in the wide range of NGT's compared to the apparent uniformity, or narrow range $\delta^{18}O$ and δ^2H isotopes around depleted values.

An NGT higher than measured water table temperatures would require one of the following: 1) water tables in recharge areas being shallow enough to reflect seasonal air temperature changes (unlikely in arid areas), and recharge to only occur during warmer months (which is not evidenced by stable isotope signatures of waters sampled in this study), 2) a deep, geothermally heated water table in mountainous areas where water has low salinities. Wells at the Bonneville Salt Flats reflect calculated geothermal gradients of 40–70 °C/km, similar to expected geothermal gradient for the Basin and Range Province (Smith et al., 2011; Coolbaugh et al., 2005). Assuming this geothermal gradient in the recharge area, the water table would need to be 150–250 m deep to gain the 10 °C elevated temperatures seen at the mesothermal

springs in this study. This is unlikely because there are high elevation springs which discharge at the measured water table temperatures of 11 °C (Gardner and Heilweil, 2014) or cooler temperatures. Or, 3) waters have equilibrated with air at elevated salinities and low, basin-level elevations.

Blue Lake, Lookout Point, and Bonneville Salt Flat samples generally had lower concentrations of each noble gas than other samples in the region, as may be expected for saline waters in equilibrium with the atmosphere (Aeschbach-Hertig et al., 1999; Stute and Schlosser, 1993; Smith and Kennedy, 1983). Wells on the Bonneville Salt Flats have depths of 3.7, 29, and 91 m and have high salinities, from 14 to 234 mS/cm (~10–200‰). NGTs for these samples modelled with 0 and 0.25‰ recharge salinities have unacceptably high $\Sigma\chi^2$ values and yield recharge temperatures > 30 °C. Thus, these samples were modelled without fractionation but with the additional parameter of variable salinity to account for potential mixing of saline recharge waters.

The samples suspected of saline recharge conditions were modelled without fractionated excess air conditions, but with variable salinities. The following scenarios were considered: Hypothesis 1/2: if mountain-front recharge occurred, whether in the Goshute-Toano Range (Hypothesis 1) or the Deep Creek Range (Hypothesis 2), the elevation would be the same used for the NGT_{avg} models. The recharge water would be fresh, with salinity variable from 0 to 1.5‰. The elevated temperature found in the closed system equilibrium models reflect the depth of the water table as would be required to geothermally heat the groundwater system there from the measured water table temperatures of 11 °C in the mountains (Gardner and Heilweil, 2014). Hypothesis 3: direct lacustrine infiltration from a desiccating lake. Elevation would be at the bottom of the basin (the sampling elevation), and temperature would be near the measured water table temperatures (variable up to 30 °C for the shallow Bonneville Salt Flats brines to reflect seasonality from the shallow water table), which was modelled to be variable from 14 to 18 °C. Salinity was modelled to vary from 0‰ to the sample salinity.

Fig. 8B shows the difference in $\Sigma\chi^2$ values for the model fits for these two recharge scenarios. For the playa-margin springs at Fish Springs and Blue Lake, samples fit much better to Hypothesis 1/2, of mountain-front recharge. Hypothesis 1/2 NGTs at BL are elevated to 19.8–23.9 °C and Fish Springs to 18.1–16.5 °C. These model fits require a water table depth of > 100 m assuming a minimum geothermal gradient of 40 °C/km. Mid-playa shallow brines at the Bonneville Salt Flats yield poor model fits for both scenarios ($\Sigma\chi^2 \gg 6.64$), although there are smaller $\Sigma\chi^2$ values for the lacustrine infiltration models of Hypothesis 3 than for Hypothesis 1/2. The deep brine at the Bonneville Salt Flats (well depth of 91 m) does not have a good fit for either scenario, but the Hypothesis 1/2, mountain-front recharge has a lower $\Sigma\chi^2$ ($\Sigma\chi^2_{\text{Scenario 1}} = 8.52$, $\Sigma\chi^2_{\text{Scenario 2}} = 15.14$).

3.5. Strontium isotopic ratios: constraint on water/rock interaction

Radiogenic ^{87}Sr abundance is compared to that of stable ^{86}Sr, and the $^{87}Sr/^{86}Sr$ ratio varies due to the ^{87}Rb content of rocks, and as a function of rock age and time of rock weathering (Fig. 9). Granitic and other felsic rocks incorporate Rb in higher concentrations and are associated with $^{87}Sr/^{86}Sr$ ratios of over 0.711 (Capo et al., 1998). Mafic igneous rocks (continental or oceanic) can have a wide range of $^{87}Sr/^{86}Sr$ ratios (0.702–0.714) (Capo et al., 1998; Faure, 1986). Limestone rocks generally have Sr isotope ratios between 0.708 and 0.710, reflecting ocean chemistry at the time of deposition, where the higher values correspond to older rocks (Whitney and Hurley, 1964; Bataille and Bowen, 2012). Dissolution of gypsum evaporites could also contribute strontium in groundwater. Groundwater will retain a specific range of $^{87}Sr/^{86}Sr$ ratios derived from each of these aquifer materials the rocks it has equilibrated with.

Blue Lake and other playa-margin springs (excluding Staley Spring) have elevated $^{87}Sr/^{86}Sr$ from 0.7131 to 0.7137, which is higher than would be expected for interaction with carbonate aquifer material (Fig. 9). Sr concentrations are 2.47 mg/L at Blue Lake, 1.74 mg/L at Fish Springs, and 0.31 mg/L at Redden Spring. These ratios are similar to groundwaters in Bear River and the Great Salt Lake (0.7200 and 0.7147, respectively) (Bright et al., 2009; Hart et al., 2004; Jones and Faure, 1972). The higher value at the Great Salt Lake has been attributed to chemical weathering of volcanic rocks (Hart et al., 2004), which may be the same mechanism for elevated $^{87}Sr/^{86}Sr$ ratios in the playa-margin springs.

The mid-playa groundwaters have $^{87}Sr/^{86}Sr$ ranges from 0.7117 to 0.7127 and concentrations from 26 to 50 mg/L. These are $^{87}Sr/^{86}Sr$ ratios lower than the playa-margin springs. Evolution from the playa-margin springs to the mid-playa brines does not fit a linear model (Fig. 9). Staley Spring discharges about 1 km inward from the playa margin, has a relatively low Sr concentration (0.72 mg/L) and has a $^{87}Sr/^{86}Sr$ value of 0.7125, which is more characteristic of mid-playa groundwater than a playa-margin spring.

Groundwaters sampled in the Deep Creek Valley and the Goshute-Toano Range generally have $^{87}Sr/^{86}Sr \leq 0.711$, which is expected of the carbonate and alluvial basin-fill aquifers (Whitney and Hurley, 1964; Bataille and Bowen, 2012). Samples from Johnson Canyon Spring and surface waters of the Deep Creek Range; however, have $^{87}Sr/^{86}Sr \geq 0.712$, which may be due to weathering of more radiogenic minerals in the granitic and meta-sedimentary rocks of the Deep Creek Range. From these sources, as Deep Creek flows northward towards Blue Lake over alluvial basin-fill, it decreases in its $^{87}Sr/^{86}Sr$ ratio to 0.711, a value significantly lower than observed at Blue Lake (Fig. 9).

4. Discussion

Each of the methods employed are used to evaluate the three hypotheses of groundwater flowpaths discharging at Blue Lake. Discharge at Blue Lake may be from mountain-front recharge, (Hypothesis 1), interbasinal groundwater flow (Hypothesis 2), or lacustrine recharge from piedmont aquifers (Hypothesis 3). Water may also represent a mixture of these recharge sources. Analytical methods to constrain the provenance and flowpaths are summarized in Table 1.

4.1. Mountain-front recharge

Hypothesis 1, mountain-front recharge, is the geologically simplest explanation for supplying water to Blue Lake. Major ion composition of Blue Lake waters largely reflects dissolution of playa evaporites, but the total solute concentration is much less than mid-playa groundwaters. Blue Lake water may be discharging from flowpaths chemically evolving from the higher mountain-front recharge areas towards the playa (Hypothesis 1 or 2).

Radiocarbon ages of the discharge at Blue Lake suggest that mean transit time is 5–12 ka. Flowpaths modelled as originating from the Goshute-Toano Range in the GBCAAS model (Brooks et al., 2014) are on the shorter end of this range, averaging 5.9 ka, making Hypothesis 1 a viable option for supplying water to Blue Lake.

Although little is known about the production of terrigenic SF_6, it has been suggested by Harnisch and Eisenhauer (1998) and Koh et al. (2007) that it is associated with igneous aquifer material and also can be accumulated in sedimentary basins. Here, SF_6 accumulates in the Bonneville basin, and the only potential recharge area with similarly high SF_6 concentration in our samples is at Mud Springs in the Goshute-Toano Range, not in the Deep Creek Valley. Thus, SF_6 accumulation likely represents connectivity of flowpaths between the Goshute-Toano Range and Blue Lake (Hypothesis 1, mountain-front recharge).

The water samples in the mountain-front springs in the Goshute Toano Range as well as the alluvial aquifer of the Deep Creek Valley do not exhibit elevated $^{87}Sr/^{86}Sr$ ratios, which does not support the hypothesis that Blue Lake is supplied only by Hypothesis 1, mountain front recharge, or the shallow aquifer of the Deep Creek Valley.

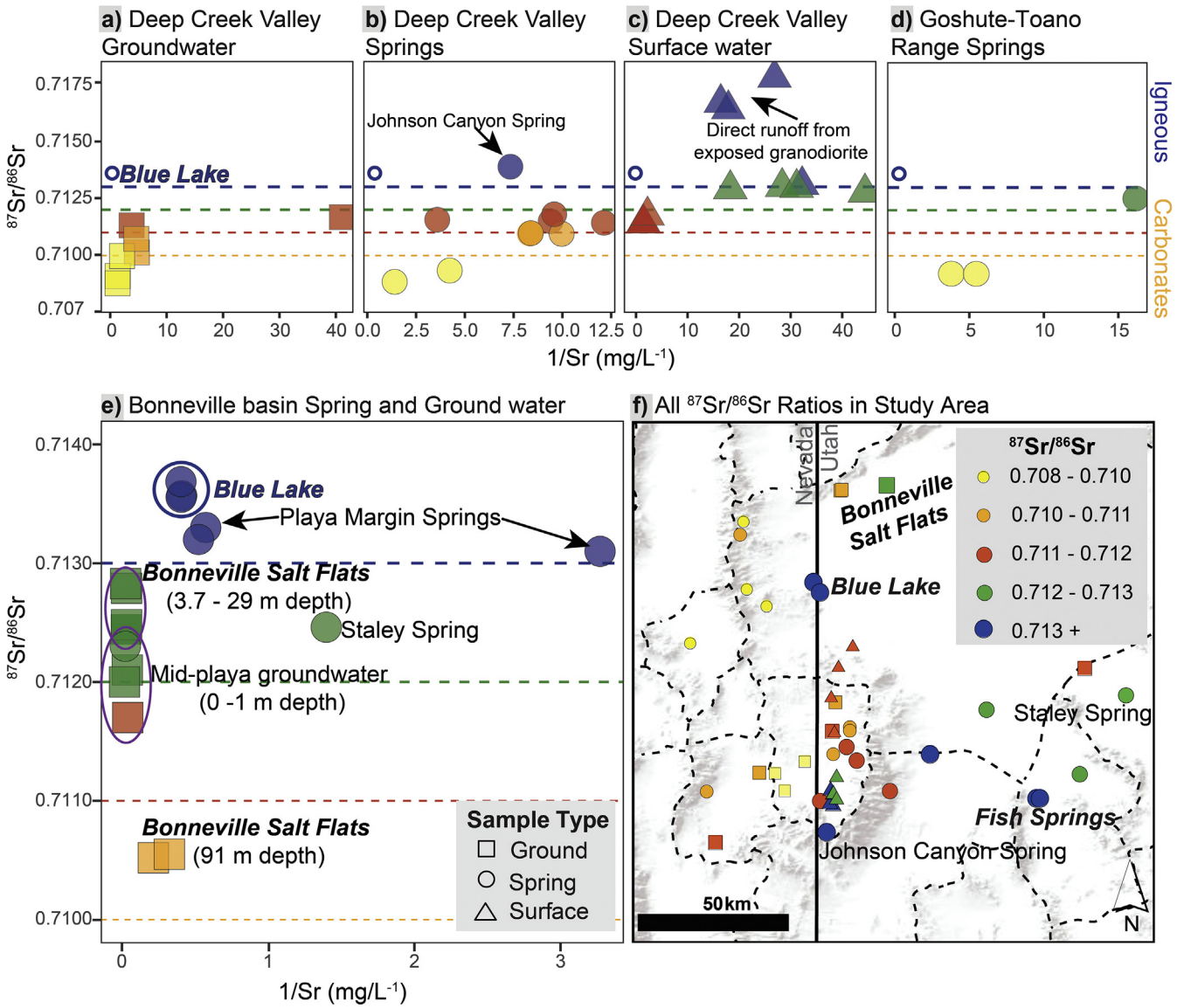

Fig. 9. Strontium isotopic composition. a–e) $^{87}Sr/^{86}Sr$ ratio versus the inverse of concentration in mg/L for regions or sample types within the study area. Horizontal dashed lines help differentiate between hypothesized rock types. Values above 0.7130 likely represent igneous aquifer materials, whereas values 0.7080–0.7100 represent carbonate-dominated aquifer materials. Samples from the Deep Creek Valley represent possible flowpaths in Hypothesis 2, interbasinal Flow. Samples from the Goshute-Toano Range represent Hypothesis 1, mountain-front recharge. f) Location map of samples analyzed for strontium isotope composition, sized by isotope $^{87}Sr/^{86}Sr$ ratio.

Using our generalized water budget, a steady-state recharge system using modern recharge rates may not supply enough water volume to account for the amount of discharge occurring at Blue Lake, as the modelled discharge from Blue Lake > 50% of the estimated recharge calculated for PRA1 (Fig. 3, Table 1). Invoking climatic changes and the associated changes in recharge rate could balance the water budget, but specifically evaluating transience in this groundwater system is beyond the scope of this study. Additional recharge to Blue Lake can also be theoretically gained from additional, longer flowpaths from other basins as described by Hypothesis 2.

4.2. Interbasinal groundwater flow

Hypothesis 2, interbasinal groundwater flow, can supply additional water to Blue Lake under an assumption of steady-state, but there may be structural controls that reduce the connectivity between basins (Nelson and Mayo, 2014 and references therein).

Because this regional aquifer system is largely comprised of carbonate and alluvial basin-fill, it is likely that there are a wide range of flowpath lengths from both the Deep Creek and Goshute-Toano Ranges converging at Blue Lake, with an average transit time well within the window of modelled radiocarbon transit times of 5–12 ka. We allow for some conjecture that a past cooler climate than exists today could have supplied relatively higher recharge rates, thus allowing a transient system to supply water to Blue Lake today.

The accumulation of high ^{4}He and low R/R_a ratios at Blue Lake are not seen at any other groundwater sites in the Bonneville basin and other sites with similar dissolved helium are south of Fish Springs along the north-south trending playa margin. These data suggest that accumulated He is entrained in upwards-moving long flowpaths that are consistent with Hypothesis 2, interbasinal flow.

Elevated $^{87}Sr/^{86}Sr$ ratios above 0.711 are only seen in samples interacting with granitic and meta-sedimentary rocks of the Deep Creek Range (Johnson Canyon Spring, Deep Creek surface waters), supporting Hypothesis 2, that of interbasinal groundwater flow. Dissolution of these radiogenic aquifer materials may be contributors of both the high

Table 1
Summary matrix of analyte interpretations within the context of tested hypotheses.

Analysis	Summary	Hypothesis 1: mountain-front recharge	Hypothesis 2: interbasinal flow	Hypothesis 3: lacustrine infiltration
Remote sensing	BL represents 50–64% of the recharge budget of PRA1, and 7–9% of the recharge calculated for PRA3.	x	x	
Field parameters	Blue Lake is warmer and more solute-laden than most spring waters in the region of study. Blue Lake is similar to other playa-margin springs in temperature and salinity.	x	x	
Major ions	Blue Lake water is an Na-Cl type water, along with other playa margin springs and Bonneville Basin waters.	x	x	x
Stable oxygen and hydrogen isotopes	Blue Lake looks like a seasonally averaged water, closely related to groundwaters and springs in the West Desert regardless of elevation.	x	x	x
Carbon and tritium	The mean transit time for water at Blue Lake is 5–12 ka, likely longer than the flowpaths estimated from the GBCAAS model coming from the Goshute-Toano Range.	x	x	
Sulfur hexafluoride	Terrigenic production of SF_6 found at Blue Lake is only seen elsewhere at the Bonneville Salt Flats and in the Goshute-Toano Range.	x		
Helium	Long accumulation time and some mantle degassing results in a low R/R_a value and high He cm^3/g STP accumulating at Blue Lake because of an upward-bound flowpath.	x	x	
Noble gasses	BL recharged in warm, fresh conditions, possibly at a geothermally heated water table at higher elevations.	x	x	
Strontium	BL and other playa-margin springs have elevated strontium concentrations and $^{87}Sr/^{86}Sr$ ratios, unlike mid-playa brines or groundwaters in adjacent basins. BL and playa-margin springs.		x	

rubidium and potassium concentrations in the Bonneville basin, which is particularly relevant as the mining at the Bonneville Salt Flats is of KCl (Bowen et al., 2018).

Although the water at Fish Springs is likely younger than the water at Blue Lake on the basis of radiocarbon, the elevated $^{87}Sr/^{86}Sr$ ratios are almost identical, suggesting that these spring systems reacted with similar rock types. As the playa-margin springs have higher $^{87}Sr/^{86}Sr$ ratios than the mid-playa brines, it is possible that interaction with deeper, more radiogenic aquifer materials, supplying the more radiogenic $^{87}Sr/^{86}Sr$ signatures.

4.3. Lacustrine infiltration

Hypothesis 3, lacustrine recharge of piedmont aquifers, has been suggested to occur, explaining sedimentary evidence of anoxic layering within the Great Salt Lake by the addition of cold, fresh groundwater (Oviatt et al., 2015). The results presented here suggest that this is an unlikely scenario in the western Bonneville basin because, 1) the geothermal gradient in the Bonneville basin would be expected to provide discharge warmer than the mean annual temperature at Blue Lake, Fish Springs and other playa-margin springs; 2) persistent wetland sediment accumulation in sediment cores at Blue Lake provides evidence of relatively stable discharge over the last 15 ka (Louderback and Rhode, 2009). If a lake was the main mechanism for recharge into the aquifer, there would be an initially higher hydraulic gradient, and thus more discharge just after the desiccation of the lake with a gradual decrease in discharge over time. Paleoenvironmental interpretations from cores do not provide evidence for this transient response.

The δ^2H and $\delta^{18}O$ values in Blue Lake and other playa margin springs are well within the range expected for modern groundwater. If these springs were recharged by waters solely of a colder-climate Pleistocene lacustrine environment, they would likely be more depleted than observed.

Comparison of radiocarbon ages at Blue Lake to Fish Springs suggests that flowpath geometry and distribution plays a role in the storage of groundwater from various time periods. The difference in groundwater mean transit time in these two systems indicates that recharge occurred in multiple time periods, and these playa springs are not all related to Hypothesis 3, a single lacustrine recharge event. The wide range of mean transit times seen in radiocarbon values in three pools at Fish Springs additionally suggests a wide range of flowpaths that converge at this location, and not a single recharge event.

The noble gas compositions suggest that Hypothesis 3, lacustrine infiltration, as a mechanism of recharge to the playa-margin springs was unlikely. Mid-playa shallow brines in the Bonneville basin likely experience saline recharge conditions, but these might be due to a hydrogeologically separate shallow aquifer system, rather than regional infiltration. Other waters, including Blue Lake, likely experienced warm, fresh, high elevation recharge conditions. This type of recharge could allow for either recharge in the Goshute-Toano Range (Hypothesis 1) or via interbasinal flow (Hypothesis 2). The elevated NGTs for playa-margin springs indicate that there may be geothermal heating at the water table in recharge areas.

The measured $^{87}Sr/^{86}Sr$ values of Blue Lake (0.7136–0.7137) and other playa-margin springs (including Fish Springs) (0.7125–0.7133) are substantially higher than documented $^{87}Sr/^{86}Sr$ ratios for Lake Bonneville carbonates (0.7113–0.7118) (Fig. 9) (Pedone and Oviatt, 2013; Hart et al., 2004). They are more similar to the $^{87}Sr/^{86}Sr$ of the Great Salt Lake during the Gilbert Wet Episode and the modern Great Salt Lake, which are thought to have become higher due to input of radiogenic, and Sr-rich waters from the Bear River (Oviatt, 2014; Hart et al., 2004). It is unlikely that waters of the Great Salt Lake are physically connected to the playa-margin springs because the relatively flat potentiometric surface in the Bonneville basin does not indicate significant potential for flow or mixing. What is more hydrologically likely is that the transition to higher $^{87}Sr/^{86}Sr$ ratios in the Great Salt Lake is

due to a transition to water and solute inputs to the lake, including high $^{87}Sr/^{86}Sr$ playa-margin springs and/or surface waters. Regardless, the high $^{87}Sr/^{86}Sr$ ratios of the playa-margin springs also do not support Hypothesis 3, lacustrine infiltration.

The strontium isotope data presented here may differentiate the provenance of playa-margin, mid-basin, and other groundwaters in the region when placing them in the context of human behavioral ecology in the eastern Great Basin during the Pleistocene-Holocene transition. Pleistocene-Holocene human foragers practiced a subsistence strategy heavily focused on wetlands (Elston et al., 2014) that were present at locations such as Blue Lake, Fish Springs, the Old River Bed Inland Delta, and Redden Springs (Schmitt and Lupo, 2018; Oviatt and Shroder, 2016; Madsen, 2016; Goebel et al., 2011; Louderback et al., 2011). With the $^{87}Sr/^{86}Sr$ groups identified in this study, $^{87}Sr/^{86}Sr$ ratios of cultural materials such as carbonate shells at rock shelters could be utilized to identify water sources that might have been used by Pleistocene-Holocene foragers and highlight any land-use patterns.

5. Conclusion

This study presents an updated water budget for Blue Lake wetlands and spatial analyses of radiocarbon derived groundwater transit times, noble gas recharge conditions, helium isotope evolution, and strontium isotope characterization of waters in Utah's West Desert. Based on our interpretations of these data, we posit that springwater at Blue Lake likely is the final discharge point of freshwater aquifers recharged as mountain-front recharge in the Goshute-Toano and interbasinal groundwater flow through the Deep Creek Valley (Hypotheses 1 and 2). In the proposed scenario, water interacting with granitic intrusions in deep basinal aquifers resulted in the unique playa-margin spring strontium isotopic compositions. It is unlikely that water discharging at Blue Lake is lacustrine infiltration from Lake Bonneville (Hypothesis 3). As such, it is likely that a combination of Hypotheses 1 and 2 can be used to explain similar observations at other playa-margin springs as well.

Acknowledgements

We acknowledge that this study was conducted on traditionally Newe/Western Shoshone and Goshute lands and express our deepest appreciation. We thank University of Utah undergraduate students who participated as field and lab assistants: Hannah Stinson, Emily Kam, Sean Hutchings and Mark Radwin. This research was supported by the Global Change and Sustainability Center at the University of Utah, Geological Society of America Graduate Student Research Award, a NSF Coupled Natural Human Systems (Award #1617473) to Bowen, and the U.S. Geological Survey in cooperation with the Bureau of Indian Affairs and the U.S. Bureau of Land Management. Strontium data for Fish Springs and from Dugway was obtained with the support of the IMWU-PWE (Environmental Programs) section of the Dugway Cultural Resource Office and the United States Army as part of ongoing research. We are thankful for the thoughtful comments by internal USGS pre-publication reviewer John Solder and anonymous reviewers. Thank you to Phil Gardner of USGS for facilitating access to public data and for research discussions.

Appendix A. Water budget

Recharge estimates were extrapolated from the Basin Characterization Model for the Great Basin Carbonate and Alluvial Aquifer System of Nevada, Utah, and Parts of Adjacent States (Flint et al., 2011). Direct Recharge and Runoff were quantified by using the sum of modelled pixel values for the specified area encompassing the Goshute-Toano Range. Results from this model extraction were adjusted according to recommendations in Chapter D of the Conceptual model of the GBCCAS (Heilweil and Brooks, 2010) by accounting for infiltration from runoff as runoff * 0.10 and adding that to the direct recharge parameter.

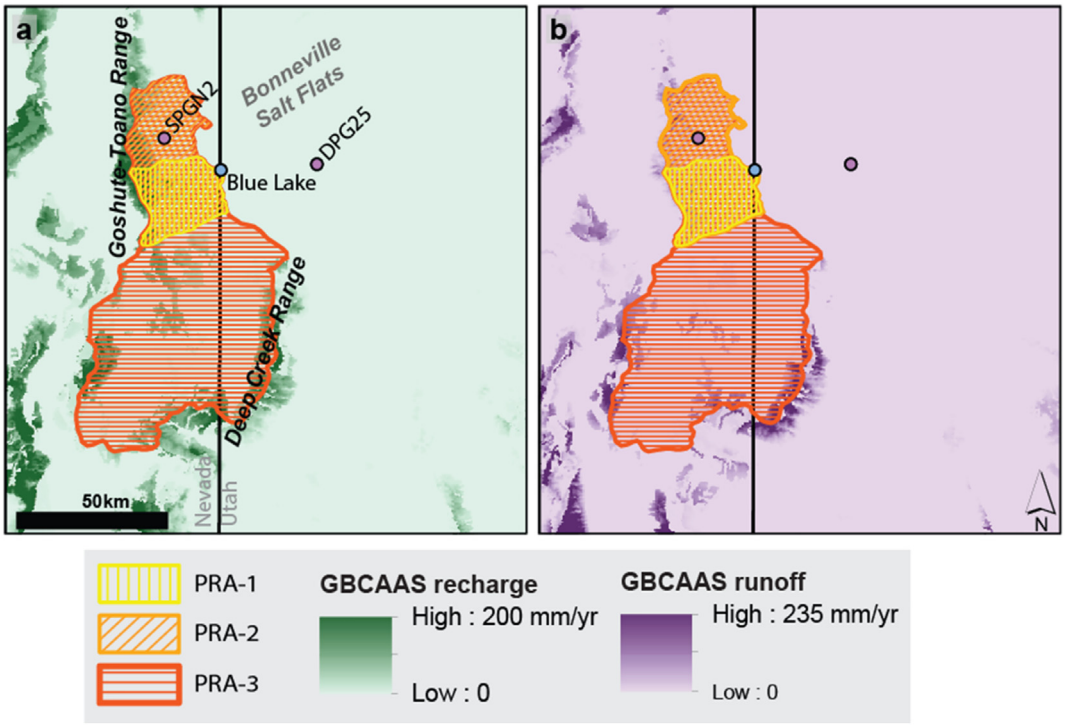

Fig. A.1. Maps of recharge, and runoff rasters used by the GBCAAS model (Brooks et al., 2014) with Proposed Recharge Area boundaries (PRA1–3).

We used LANDSAT-based imagery to quantify the Blue Lake marshland area and applied estimates of ET rates measured by Welch et al. (2007) to estimate the discharge rate of water from the Blue Lake system. Each image was resized to the largest Blue Lake footprint found in the images. Images

were not co-located due to negligible observable differences and lack of control points due to morphological changes in the natural landscape.

Using each image, NDVI and NDWI thresholds of −0.160 and −0.004, respectively, were determined to be a most conservative estimate of vegetation and open water without encompassing the reflectance values of meadowland and grasses associated with rain events, or reflectance of playa evaporites. The scenes collected had no cloud cover over the Blue Lake footprint area. The average number of pixels above the NDVI threshold is 11,825,527 pixels (σ = 6048). Variation of area is likely due to temperature fluxes, as the smallest areas are in fall and winter when temperatures have been particularly low, and plants may be dormant. The average number of pixels above the NDWI threshold is 191 pixels (σ = 332). Pixel resolution of these scenes is 900 m^2.

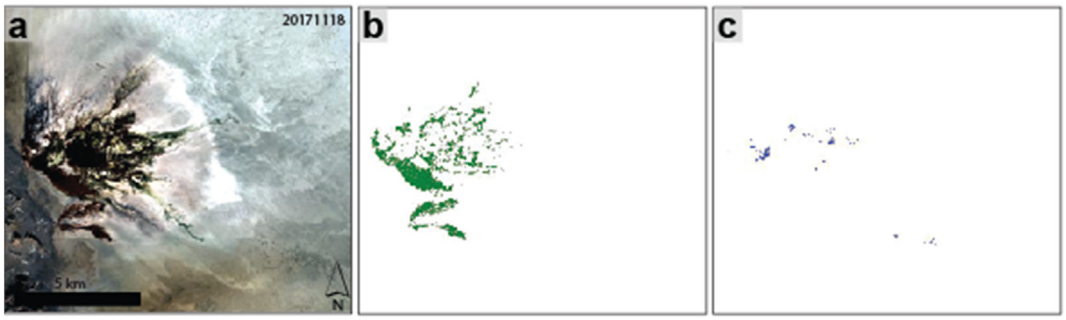

Fig. A.2. Examples of NDVI and NDWI thresholds over the Blue Lake study area from November 19, 2017.

Appendix B. Major and trace element collection

The major ion composition and select trace elements in water samples were used to characterize water quality and evaluate potential flowpaths. Samples to be analyzed for major ions were collected in High-Density Polyethylene (HDPE) bottles 125 mL to 500 mL bottles (VWR catalogue 89221-662) that were triple rinsed with Millipore Academic A10 Milli-Q water (MQW). Samples had minimal headspace and were filtered with a 0.45 μm polypropylene syringe filter. Samples were sealed with Parafilm. Titrations are reported mg/L as $CaCO_3$ using the fixed endpoint method (Brooks et al., 2014).

Ion chromatography was analyzed by Activation Laboratories Ltd. or USGS National Water Quality Laboratory. Samples yielded charge balances of < 10%. Samples collected in acid washed 3 L HDPE bottles and subsampled according to the USGS National Field Manual guidelines (Wilde and Radtke, 1998).

ICP-MS bottles were acid washed with 5% HCl, rinsed with MQW and dried in a dust free environment. Sample bottles were rinsed with sample once before filling with minimal headspace. Samples were filtered in the field with sterile cellulose acetate sterile syringe filters (VWR catalogue 28145-481) kept at 20 °C without preservative. Samples collected with the USGS were subset from 3 L acid washed HDPE bottles.

Samples were analyzed by University of Utah's Strontium Isotopes Laboratory for trace elements and $^{87}Sr/^{86}Sr$ isotope ratios using a multi-collector inductively coupled plasma mass spectrometry (ICP-MS) on a Thermo Scientific Neptune. Strontium isotope ratios of all samples used the SrFast method (Mackey and Fernandez, 2011).

Appendix C. Stable oxygen and hydrogen isotopes

Water stable isotopes ($\delta^{18}O$ and $\delta^{2}H$) were used to understand the sources and source conditions of groundwater when it fell as precipitation. Samples were analyzed on the same samples analyzed for major ions, and subset when the bottles were first opened, to prevent evaporation. These were subsampled into 1.8 mL glass gas chromatography crimpseal vials. Samples were analyzed using a Picarro L2130-i $\delta^{18}O/\delta^{2}H$ Ultra High Precision Isotopic Water Analyzer at the Stable Isotope Ratio Facility for Environmental Research laboratories. These facilities cryogenically extracted water from samples with specific conductances > 20,000 μS/cm.

Appendix D. Radiocarbon

Radiocarbon (^{14}C) is used in groundwater dating as an inaccurate but useful tool (Han and Plummer, 2016) to understand relative ages of waters known to react along similar pathways. Precise ^{14}C ages are difficult to ascertain, because of the complex reaction pathways that groundwater undergoes. All samples were kept refrigerated and used an overflow method, where bottles with sampling tube at the bottom were placed underwater in a 5 gal thoroughly rinsed plastic bucket and overfilled with filtered sample water for at least 3 bottle volumes. USGS samples used 1 L glass bottles sealed with electrical tape.

Samples collected by the University of Utah were collected in 500 mL glass bottles with a 29/26 standard taper ground glass joint and solid glass stopper. These sample bottles were acid washed, washed and stored according to Woods Hole Oceanographic Institution specifications. The stopper was coated with Apiezon-M high vacuum grease and twisted into the bottle neck to ensure a good seal. No ^{14}C samples were poisoned.

^{14}C and $\delta^{13}C$ samples were analyzed by the National Ocean Sciences Accelerator Mass Spectrometer facility at Woods Hole Oceanographic Institution. ^{14}C was reported as specified by Stuiver and Polach (1977) and $\delta^{13}C$ was reported relative to the Pee Dee Belemnite (PDB) standard.

^{14}C in groundwater samples but be corrected to translate an activity to an apparent age. These modelled ages themselves, are useful to represent a relative mean transit time of water but does no account for mixtures of flowpaths with different radiocarbon activities, and corrections for reservoir effects and soil carbon exchange introduces additional error. Three models were used in this study to provide bracketed apparent ages, correcting for soil carbon exchange and water-rock exchange in the subsurface. All samples were treated with the same equations, assuming the water rock interactions would affect all samples in the study area. Modelled values for solid-rock endmembers ^{14}C, $\delta^{13}C$ were 0. Tamers' Model (Eq. (D.1)) (Han and Plummer, 2016; Tamers, 1975; Tamers and Scharpenseel, 1970; Tamers, 1967) was used as a preliminary and underestimate of apparent age. A version of Fontes and Garnier's Model (1979) corrected by Han and Plummer (2013) (Han and Plummer, 2016) (Eq. (D.2)) and the IAEA (Han and

Plummer, 2016; Salem et al., 1980; Gonfiantini, 1972) (Eq. (D.3)) models were used to create an upper and more accurate bracket or apparent ages. These modelled ages create an estimate of radiocarbon age relative to the related samples. Specifics of the different treatment models are discussed thoroughly in Han and Plummer, 2016, and therefore will not be discussed here. We note that a 2‰ difference in the $\delta^{13}C$ value leads to an average difference of 750 years in the Han and Plummer (2013) model and 1300 years in the IAEA model.

$$^{14}C_0 = (C_a/C_T)^{14}C_g + 0.5\,(C_b/C_T)(^{14}C_g + {}^{14}C_s) = T \quad \text{(D.1)}$$

where:

$^{14}C_0$ = Initial carbon isotopic composition of DIC adjusted for geochemical reactions without decay (pMC)
C_a = Concentration of $CO_{2(aq)}$ (mol/kg)
C_T = Total concentration of dissolved inorganic carbon ($C_a + C_b$) (mol/kg)
$^{14}C_g$ = Carbon isotopic composition of dissolved soil CO_2 in equilibrium with soil gas CO_2 (pMC)
C_b = Concentration of HCO_3^- (mol/kg)
$^{14}C_s$ = Carbon isotopic composition of solid carbonate minerals (pMC)

$$^{14}C_0 = T + (^{14}C_x - {}^{14}C_i - 0.2\varepsilon_{x/b})\,((\delta^{13}C_{DIC} - (C_a/C_T)\delta^{13}C_{a1} - (C_b/C_T)\delta^{13}C_i)/(\delta^{13}C_x - \delta^{13}C_i - \varepsilon_{x/b})) \quad \text{(D.2)}$$

where:

T = (Eq. (D.1))
$^{14}C_x$ = Carbon isotopic composition of dissolved carbon coming from solid carbonate (pMC)
$^{14}C_i$ = 'Primary' carbon isotopic composition of DIC (pMC)
$\varepsilon_{x/b}$ = ^{13}C fractionation factor of carbonate mineral with respect to HCO_3^-
$\delta^{13}C_{DIC}$ = Carbon isotopic composition determined from the sample (‰)
$\delta^{13}C_{a1}$ = Carbon isotopic composition of dissolved soil CO2 in equilibrium with soil gas CO_2 (‰)
$\delta^{13}C_i$ = 'Primary' carbon isotopic composition of DIC (‰)
$\delta^{13}C_x$ = Carbon isotopic composition of dissolved carbon coming from solid carbonate (‰)

$$^{14}C_0 = ((^{14}C_g\delta^{13}C_{DIC})/(\delta^{13}C_g + \varepsilon_{b/g}))(1 + (2\varepsilon_{b/g}/1000)) \quad \text{(D.3)}$$

where:

$^{14}C_g$ = Carbon isotopic composition of dissolved soil CO_2 in equilibrium with soil gas CO_2 (assumed to be 100) (pMC)
$\delta^{13}C_g$ = Carbon isotopic composition of dissolved soil CO_2 in equilibrium with soil gas CO_2 (‰)
$\varepsilon_{b/g} = -1\,(\varepsilon_{g/b}) = -1$ (^{13}C fractionation factor of gaseous CO_2 with respect to HCO_3^-)

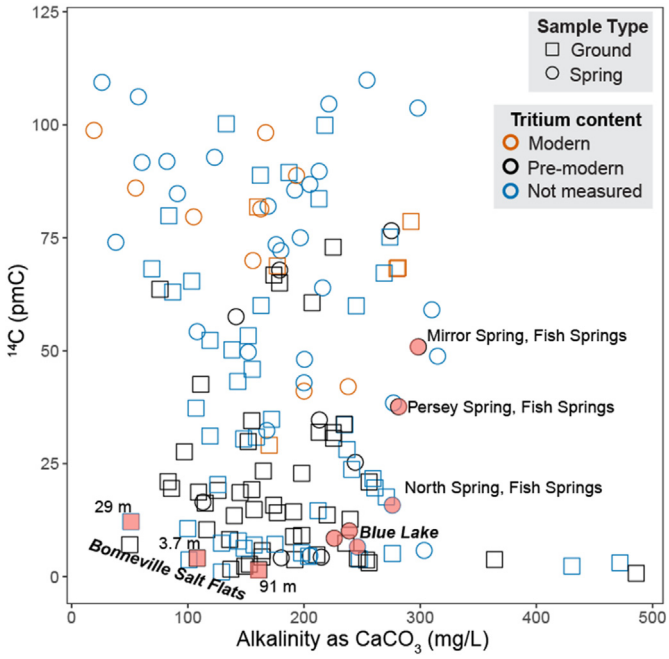

Fig. D.1. As Suggested by Han et al. (2012) a plot of radiocarbon content vs. alkalinity is shown here to graphically observe the evolution of carbonate isotopes.

Appendix E. Tritium

Tritium was used to determine the component of modern recharge of waters sampled. These samples were collected in Low-Density Polyethylene (LDPE) 1 L bottles sealed tightly with minimal headspace. Samples stored for over 1 month were sealed with electrical tape. Samples were analyzed at University of Utah Dissolved and Noble Gasses Laboratories using the helium in-growth methodology over 6+ months, and distillation was performed for samples with specific conductance > 100,000 µS/cm. Reported error was ± 2% of value with a detection limit of 0.05 TU.

Appendix F. Noble gasses

Dissolved gasses were sampled at Blue Lake and the surrounding areas in 2017–2018. The concentrations and proportions of noble gasses Ne, Ar, Kr, Xe, ^{4}He, and $^{3}He/^{4}He$ were used to evaluate possible temperatures and elevations at which water last interacted with the atmosphere, presumably where the water recharged from the vadose to saturated zone. These ratios help to calibrate other dissolved gas tracers for excess air. Helium isotopes are useful to evaluate terrigenic sources of helium, such as from Ur-Th decay or from mantle degassing (Genereux et al., 2009; Wiersberg and Erzinger, 2007; Crossey et al., 2006; Solomon and Cook, 2000). Samples were collected with refrigeration-grade copper tubing (0.95 cm OD by 70 cm long). Water was pumped through polyethylene tubing and a peristaltic pump connected to the copper tube which was angled upwards and tapped with a wrench to remove potential bubbles. Positive pressure was maintained on the outflow polyethylene tube while the copper tube was sealed with metal pinch clamps to avoid gas exsolution. Reported measurement error for helium is ± 1% of value, and ± 1% to 5% of value for all other gasses.

The noble gas isotopes Xe, Kr, Ar, and Ne were used in a closed-system equilibration model to estimate the recharge temperature (Kipfer et al., 2002; Aeschbach-Hertig et al., 2000). This model estimates the amount of excess air (Ae) trapped at the water table and the fractionation factor of that air, if it is wholly or partially dissolved.

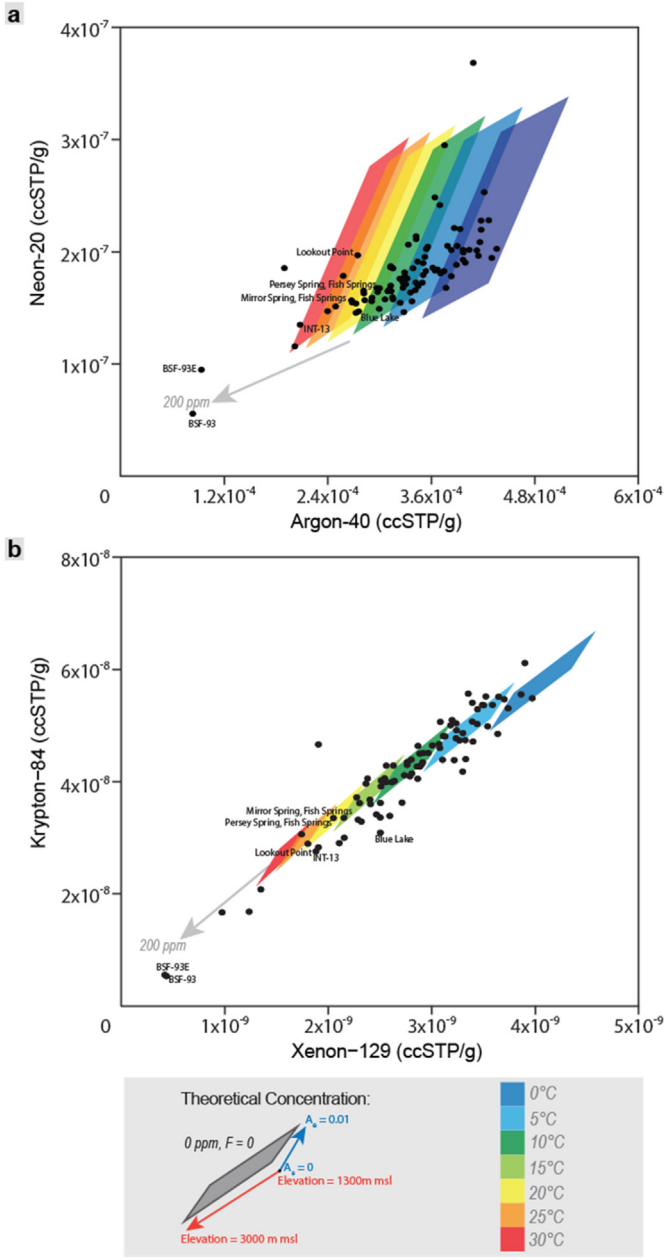

Fig. F.1. Noble gas concentrations of samples are shown here in the context of theoretical concentrations dependent on elevation, excess air, temperature, and salinity. a) Neon-20 vs. Argon-40 concentrations. b) Krypton-84 vs. Xenon-129 concentrations.

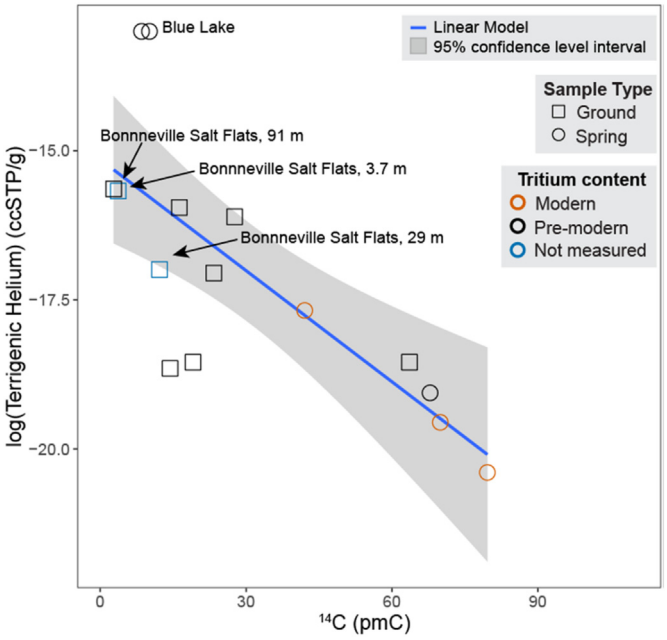

Fig. F.2. The natural log of terrigenic helium (calculated using Neon-20) vs. radiocarbon content of samples. A linear model is fit to data.

Appendix G. SF_6

Dissolved sulfur hexafluoride (SF_6) concentrations in water used in this study to evaluate relative terrigenic production as a qualitative indicator of water-rock interaction (Friedrich et al., 2013; Darling et al., 2012; von Rohden et al., 2010; Koh et al., 2007). SF_6 samples were collected for with this study and by the USGS. Samples were collected in 1-Liter sized, plastic safety coated, amber glass bottle with a polyseal cone lined cap is used. Submerged bottle was overfilled to 3× sample volume to prevent bubbles from forming in the bottle following Hunt (2015). These were analyzed using gas chromatography at University of Utah Dissolved and Noble Gasses Laboratories.

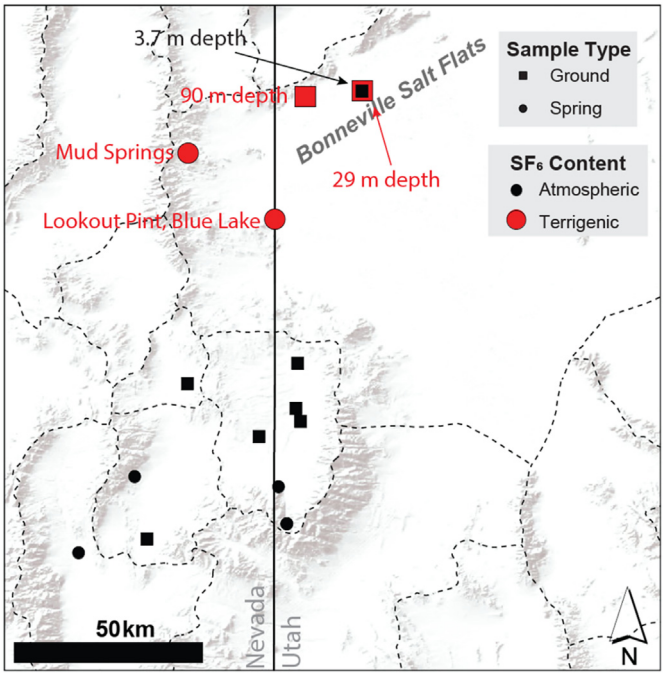

Fig. G.1. SF_6 sampling locations. Samples showing evidence of terrigenic helium production (> 9.4 pptv) are marked.

Appendix H. Supplementary data

Supplementary data to this article can be found online at https://doi.org/10.1016/j.chemgeo.2019.119280.

References

Aeschbach-Hertig, W., Solomon, D.K., 2013. Noble gas thermometry in groundwater hydrology. In: The Noble Gases as Geochemical Tracers. Springer, Berlin, Heidelberg, pp. 81–122.

Aeschbach-Hertig, W., Peeters, F., Beyerle, U., Kipfer, R., 1999. Interpretation of dissolved atmospheric noble gases in natural waters. Water Resour. Res. 35 (9), 2779–2792. https://doi.org/10.1029/1999WR900130.

Aeschbach-Hertig, W., Peeters, F., Beyerle, U., Kipfer, R., 2000. Palaeotemperature reconstruction from noble gases in ground water taking into account equilibration with entrapped air. Nature 405 (6790), 1040. https://doi.org/10.1038/35016542.

Anderson, K., Nelson, S., Mayo, A., Tingey, D., 2006. Interbasin flow revisited: the contribution of local recharge to high-discharge springs, Death Valley, CA. J. Hydrol. 323 (1–4), 276–302. https://doi.org/10.1016/j.jhydrol.2005.09.004.

Andrews, J.N., 1985. The isotopic composition of radiogenic helium and its use to study groundwater movement in confined aquifers. Chem. Geol. 49 (1–3), 339–351. https://doi.org/10.1016/0009-2541(85)90166-4.

Banerjee, A., Person, M., Hofstra, A., Sweetkind, D., Cohen, D., Sabin, A., Unruh, J., Zyvoloski, G., Gable, C.W., Crossey, L., Karlstrom, K., 2011. Deep permeable fault–controlled helium transport and limited mantle flux in two extensional geothermal systems in the Great Basin, United States. Geology 39 (3), 195–198. https://doi.org/10.1130/G31557.1.

Bataille, C.P., Bowen, G.J., 2012. Mapping 87Sr/86Sr variations in bedrock and water for large scale provenance studies. Chem. Geol. 304, 39–52. https://doi.org/10.1016/j.chemgeo.2012.01.028.

Belcher, W.R., Bedinger, M.S., Back, J.T., Sweetkind, D.S., 2009. Interbasin flow in the Great Basin with special reference to the southern Funeral Mountains and the source of furnace Creek springs, Death Valley, California, US. J. Hydrol. 369 (1–2), 30–43. https://doi.org/10.1016/j.jhydrol.2009.02.048.

Benson, L.V., Lund, S.P., Smoot, J.P., Rhode, D.E., Spencer, R.J., Verosub, K.L., Louderback, L.A., Johnson, C.A., Rye, R.O., Negrini, R.M., 2011. The rise and fall of Lake Bonneville between 45 and 10.5 ka. Quat. Int. 235 (1–2), 57–69. https://doi.org/10.1016/j.quaint.2010.12.014.

Blackett, R., Gwynn, M., Allis, R., Hardwick, C., 2013. New Utah Geothermal Data Acquisition—A Project Supporting the National Geothermal Data System.

Boutt, D.F., Hynek, S.A., Munk, L.A., Corenthal, L.G., 2016. Rapid recharge of fresh water to the halite-hosted brine aquifer of Salar de Atacama, Chile. Hydrol. Process. 30 (25), 4720–4740.

Bowen, B.B., Kipnis, E.L., Raming, L.W., 2017. Temporal dynamics of flooding, evaporation, and desiccation cycles and observations of salt crust area change at the Bonneville Salt Flats, Utah. Geomorphology 299, 1–11. https://doi.org/10.1016/j.geomorph.2017.09.036.

Bowen, B.B., Bernau, J., Kipnis, E.L., Lerback, J., Wetterlin, L., Kleba, B., 2018. The making of a perfect racetrack at the Bonneville Salt Flats. Sediment. Rec. 16 (2). https://doi.org/10.2110/sedred.2018.2.4.

Bradbury, C.D., 2019. Water Resources and Utilization in the Sevier Basin and Old River Bed Inland Delta of Central Utah During the Pleistocene-Holocene Transition. University of Utah, Dissertation.

Bright, J., Rosenbaum, J.G., Kaufman, D.S., 2009. Isotope and major-ion chemistry of groundwater in Bear Lake Valley, Utah and Idaho, with emphasis on the Bear River Range. In: Paleoenvironments of Bear Lake, Utah and Idaho, and Its Catchment. Geological Society of America, Geological Society of America Special Paper, vol. 450. pp. 105–132.

Brooks, L.E., Masbruch, M.D., Sweetkind, D.S., Buto, S.G., 2014. Steady-state numerical groundwater flow model of the Great Basin carbonate and alluvial aquifer system. In: US Geological Survey Scientific Investigation Report, pp. 124.

Busenberg, E., Plummer, L.N., 2000. Dating young groundwater with sulfur hexafluoride: Natural and anthropogenic sources of sulfur hexafluoride. Water Resour. Res. 36 (10), 3011–3030. https://doi.org/10.1029/2000WR900151.

Bushman, M., Nelson, S.T., Tingey, D., Eggett, D., 2010. Regional groundwater flow in structurally-complex extended terranes: an evaluation of the sources of discharge at Ash Meadows, Nevada. J. Hydrol. 386 (1–4), 118–129. https://doi.org/10.1016/j.jhydrol.2010.03.013.

Caine, J.S., Minor, S.A., Grauch, V.J.S., Hudson, M.R., 2002. Potential for fault zone compartmentalization of groundwater aquifers in poorly lithified, Rio Grande rift-related sediments, New Mexico. Geol. Soc. Am. Abs. 34 (4), 59.

Capo, R.C., Stewart, B.W., Chadwick, O.A., 1998. Strontium isotopes as tracers of ecosystem processes: theory and methods. Geoderma 82 (1–3), 197–225. https://doi.org/10.1016/S0016-7061(97)00102-X.

Coats, R.R., 1987. Geology of Elko County, Nevada: Nevada Bureau of Mines and Geology, Bulletin 101, scale 1:250,000.

Cook, K.L., Halverson, M.O., Stepp, J.C. and Berg Jr, J.W., 1964. Regional gravity survey of the northern Great Salt Lake Desert and adjacent areas in Utah, Nevada, and Idaho. Geol. Soc. Am. Bull., 75(8), pp.715–740. DOI:https://doi.org/10.1130/0016-7606(1964)75[715:RGSOTN]2.0.CO;2.

Coolbaugh, M.F., Zehner, R.E., Raines, G.L., Oppliger, G.L., Kreemer, C., 2005, August. Regional prediction of geothermal systems in the Great Basin, USA using weights of evidence and logistic regression in a Geographic Information System (GIS). In: International Association of Mathematical Geology Annual Conference Proceedings, Toronto, Canada, pp. 505–510.

Craig, H., 1961. Isotopic variations in meteoric waters. Science 133 (3465), 1702–1703. https://doi.org/10.1126/science.133.3465.1702.

Crossey, L.J., Fischer, T.P., Patchett, P.J., Karlstrom, K.E., Hilton, D.R., Newell, D.L., Huntoon, P., Reynolds, A.C., De Leeuw, G.A., 2006. Dissected hydrologic system at the Grand Canyon: interaction between deeply derived fluids and plateau aquifer waters in modern springs and travertine. Geology 34 (1), 25–28. https://doi.org/10.1130/G22057.1.

Darling, W.G., Gooddy, D.C., MacDonald, A.M., Morris, B.L., 2012. The practicalities of using CFCs and SF6 for groundwater dating and tracing. Appl. Geochem. 27 (9), 1688–1697. https://doi.org/10.1016/j.apgeochem.2012.02.005.

Davis, J.A., Kerezsy, A., Nicol, S., 2017. Springs: conserving perennial water is critical in arid landscapes. Biol. Conserv. 211, 30–35. https://doi.org/10.1016/j.biocon.2016.12.036.

Davisson, M.L., Smith, D.K., Kenneally, J., Rose, T.P., 1999. Isotope hydrology of southern Nevada groundwater: stable isotopes and radiocarbon. Water Resour. Res. 35 (1), 279–294. https://doi.org/10.1029/1998WR900040.

Deeds, D.A., Vollmer, M.K., Kulongoski, J.T., Miller, B.R., Mühle, J., Harth, C.M., Izbicki, J.A., Hilton, D.R., Weiss, R.F., 2008. Evidence for crustal degassing of CF4 and SF6 in Mojave Desert groundwaters. Geochim. Cosmochim. Acta 72 (4), 999–1013. https://doi.org/10.1016/j.gca.2007.11.027.

Elston, R.G., Zeanah, D.W., Codding, B.F., 2014. Living outside the box: an updated perspective on diet breadth and sexual division of labor in the Prearchaic Great Basin. Quat. Int. 352, 200–211. https://doi.org/10.1016/j.quaint.2014.09.064.

Faure, G., 1986. Isotope systematics in two-component mixtures. In: Principles of Isotope Geology, pp. 141–153.

Flint, A.L., Flint, L.E., 2007. Application of the Basin Characterization Model to Estimate In-place Recharge and Runoff Potential in the Basin and Range Carbonate-rock Aquifer System, White Pine County, Nevada, and Adjacent Areas in Nevada and Utah: U.S. Geological Survey Scientific Investigations Report 2007-5099. (20 p).

Flint, A.L., Flint, L.E., Masbruch, M.D., 2011. Input, calibration, uncertainty, and limitations of the basin characterization model: appendix three. In: Heilweil, V.M., Brooks, L.E. (Eds.), 2011, Conceptual Model of the Great Basin Carbonate and Alluvial Aquifer System: U.S. Geological Survey Scientific Investigations Report 2010-5193, (191 p).

Fontes, J.C., Garnier, J.M., 1979. Determination of the initial 14C activity of the total dissolved carbon: a review of the existing models and a new approach. Water Resour. Res. 15 (2), 399–413. https://doi.org/10.1029/WR015i002p00399.

Friedrich, R., Vero, G., Von Rohden, C., Lessmann, B., Kipfer, R., Aeschbach-Hertig, W., 2013. Factors controlling terrigenic SF6 in young groundwater of the Odenwald region (Germany). Appl. Geochem. 33, 318–329. https://doi.org/10.1016/j.apgeochem.2013.03.002.

Gans, P.B., Miller, E.L., McCarthy, J., Ouldcott, M.L., 1985. Tertiary extensional faulting and evolving ductile-brittle transition zones in the northern Snake Range and vicinity: new insights from seismic data. Geology 13 (3), 189–193. https://doi.org/10.1130/0091-7613(1985)13<189:TEFAED>2.0.CO;2.

Gardner, P.M., Heilweil, V.M., 2014. A multiple-tracer approach to understanding regional groundwater flow in the Snake Valley area of the eastern Great Basin, USA. Appl. Geochem. 45, 33–49. https://doi.org/10.1016/j.apgeochem.2014.02.010.

Gardner, P.M., Masbruch, M.D., 2015. Hydrogeologic and Geochemical Characterization of Groundwater Resources in Deep Creek Valley and Adjacent Areas, Juab and Tooele Counties, Utah, and Elko and White Pine Counties, Nevada(No. 2015-5097). US Geological Survey.

Genereux, D.P., Webb, M., Solomon, D.K., 2009. Chemical and isotopic signature of old groundwater and magmatic solutes in a Costa Rican rain forest: evidence from carbon, helium, and chlorine. Water Resour. Res. 45 (8). https://doi.org/10.1029/2008WR007630.

Gillespie, J., Nelson, S.T., Mayo, A.L., Tingey, D.G., 2012. Why conceptual groundwater flow models matter: a trans-boundary example from the arid Great Basin, western USA. Hydrogeol. J. 20 (6), 1133–1147. https://doi.org/10.1007/s10040-012-0848-0.

Goebel, T., Hockett, B., Adams, K.D., Rhode, D., Graf, K., 2011. Climate, environment, and humans in North America's Great Basin during the Younger Dryas, 12,900–11,600 calendar years ago. Quat. Int. 242 (2), 479–501. https://doi.org/10.1016/j.quaint.2011.03.043.

Gonfiantini, R., 1972. Notes on Isotope Hydrology. Internal Publication. IAEA, Vienna.

Graham, D.W., 2002. Noble gas isotope geochemistry of mid-ocean ridge and ocean island basalts: characterization of mantle source reservoirs. Rev. Mineral. Geochem. 47 (1), 247–317. https://doi.org/10.2138/rmg.2002.47.8.

Han, L.F., Plummer, L.N., 2013. Revision of Fontes & Garnier's model for the initial 14C content of dissolved inorganic carbon used in groundwater dating. Chem. Geol. 351, 105–114. https://doi.org/10.1016/j.chemgeo.2013.05.011.

Han, L.F., Plummer, L.N., 2016. A review of single-sample-based models and other approaches for radiocarbon dating of dissolved inorganic carbon in groundwater. Earth Sci. Rev. 152, 119–142. https://doi.org/10.1016/j.earscirev.2015.11.004.

Han, L.F., Plummer, L.N., Aggarwal, P., 2012. A graphical method to evaluate predominant geochemical processes occurring in groundwater systems for radiocarbon dating. Chem. Geol. 318, 88–112. https://doi.org/10.1016/j.chemgeo.2012.05.004.

Harnisch, J., Eisenhauer, A., 1998. Natural CF4 and SF6 on Earth. Geophys. Res. Lett. 25 (13), 2401–2404. https://doi.org/10.1029/98GL01779.

Harrill, J.R., Prudic, D.E., 1998. Aquifer Systems in the Great Basin Region of Nevada, Utah, and Adjacent States; Summary Report (No. 1409-A).

Hart, W.S., Quade, J., Madsen, D.B., Kaufman, D.S., Oviatt, C.G., 2004. The 87Sr/86Sr ratios of lacustrine carbonates and lake-level history of the Bonneville paleolake system. Geol. Soc. Am. Bull. 116 (9–10), 1107–1119. https://doi.org/10.1130/B25330.1.

Hart, R., Nelson, S.T., Eggett, D., 2010. Uncertainty in 14C model ages of saturated zone waters: the influence of soil gas in terranes dominated by C3 plants. J. Hydrol. 392 (1–2), 83–95. https://doi.org/10.1016/j.jhydrol.2010.08.001.

Hartigan, J.A., Wong, M.A., 1979. Algorithm AS 136: a k-means clustering algorithm. J. R. Stat. Soc.: Ser. C: Appl. Stat. 28 (1), 100–108. https://doi.org/10.2307/2346830.

Heilweil, V.M., Brooks, L.E., 2010. Conceptual model of the Great Basin carbonate and alluvial aquifer system. US Geol. Surv. Sci. Investig. Rep. 5193, 191.

Hose, R.K., Blake Jr., M.C., 1970. Geologic Map of White Pine County, Nevada (No. 70-166). US Government Printing Office.
Hunt, A.G., 2015. US Geological Survey Noble gas Laboratory's Standard Operating Procedures for the Measurement of Dissolved Gas in Water Samples (No. 5-A11). US Geological Survey.
Jones, L.M., Faure, G., 1972. Strontium isotope geochemistry of Great Salt Lake, Utah (Geological Society of America Bulletin). 83 (6), 1875–1880.
Kennedy, B.M., Van Soest, M.C., 2007. Flow of mantle fluids through the ductile lower crust: helium isotope trends. Science 318 (5855), 1433–1436. https://doi.org/10.1126/science.1147537.
Kennedy, B.M., Kharaka, Y.K., Evans, W.C., Ellwood, A., DePaolo, D.J., Thordsen, J., Ambats, G., Mariner, R.H., 1997. Mantle fluids in the San Andreas fault system, California. Science 278 (5341), 1278–1281. https://doi.org/10.1126/science.278.5341.1278.
Kipfer, R., Aeschbach-Hertig, W., Peeters, F., Stute, M., 2002. Noble gases in lakes and ground waters. Rev. Mineral. Geochem. 47 (1), 615–700. https://doi.org/10.2138/rmg.2002.47.14.
Koh, D.C., Plummer, L.N., Busenberg, E., Kim, Y., 2007. Evidence for terrigenic SF6 in groundwater from basaltic aquifers, Jeju Island, Korea: implications for groundwater dating. J. Hydrol. 339 (1–2), 93–104. https://doi.org/10.1016/j.jhydrol.2007.03.011.
Louderback, L.A., Rhode, D.E., 2009. 15,000 years of vegetation change in the Bonneville basin: the Blue Lake pollen record. Quat. Sci. Rev. 28 (3–4), 308–326. https://doi.org/10.1016/j.quascirev.2008.09.027.
Louderback, L.A., Grayson, D.K., Llobera, M., 2011. Middle-Holocene climates and human population densities in the Great Basin, western USA. The Holocene 21 (2), 366–373. https://doi.org/10.1177/0959683610374888.
Mackey, G.N., Fernandez, D.P., 2011. High throughput Sr isotope analysis using an automated column chemistry system. In: Abstract V31B-2525 Presented at 2011 Fall Meeting AGU, San Francisco, California, pp. 5–9 December.
Madsen, D.B., 2016. The early human occupation of the Bonneville Basin. In: Developments in Earth Surface Processes. vol. 20. Elsevier, pp. 504–525. https://doi.org/10.1016/B978-0-444-63590-7.00018-4.
Moore, W.J., Sorensen, M.L., 1979. Geologic Map of the Tooele 1 Degree by 2 Degrees Quadrangle, Utah (No. 1132).
National Oceanic and Atmospheric Administration, 2017. Earth System Research Laboratory Global Monitoring Division. Niwot Ridge, Colorado, United States. Data accessed. .
Nelson, S.T., Mayo, A.L., 2014. The role of interbasin groundwater transfers in geologically complex terranes, demonstrated by the Great Basin in the western United States. Hydrogeol. J. 22 (4), 807–828. https://doi.org/10.1007/s10040-014-1104-6.
Nelson, S.T., Mayo, A.L., Gilfillan, S., Dutson, S.J., Harris, R.A., Shipton, Z.K., Tingey, D.G., 2009. Enhanced fracture permeability and accompanying fluid flow in the footwall of a normal fault: the Hurricane fault at Pah Tempe hot springs, Washington County, Utah. Geol. Soc. Am. Bull. 121 (1–2), 236–246. https://doi.org/10.1130/B26285.1.
Oviatt, C.G., 2014. The Gilbert Episode in the Great Salt Lake Basin, Utah. Utah Geological Survey.
Oviatt, C.G., Shroder, J.F. (Eds.), 2016. Lake Bonneville: A Scientific Update. vol. 20 Elsevier.
Oviatt, C.G., Madsen, D.B., Miller, D.M., Thompson, R.S., McGeehin, J.P., 2015. Early Holocene Great Salt Lake, USA. Quat. Res. 84 (1), 57–68. https://doi.org/10.1016/j.yqres.2015.05.001.
Pedone, V.A., Oviatt, C.G., 2013. South to north flow in Lake Bonneville: evidence from carbonate mineralogy and geochemistry. In: Geol. Soc. Am. Abstr. Programs. vol. 45. pp. 552 October.
Pinti, D.L., Marty, B., 1998. The origin of helium in deep sedimentary aquifers and the problem of dating very old groundwaters. Geol. Soc. Lond., Spec. Publ. 144 (1), 53–68. https://doi.org/10.1144/GSL.SP.1998.144.01.05.
Rousseeuw, P.J., 1987. Silhouettes: a graphical aid to the interpretation and validation of cluster analysis. J. Comput. Appl. Math. 20, 53–65. https://doi.org/10.1016/0377-0427(87)90125-7.
Salem, O., Visser, J.H., Dray, M., Gonfiantini, R., 1980. Groundwater Flow Patterns in the Western Libyan Arab Jamahiriya Evaluated From Isotopic Data. (Groundwater flow patterns in the western Libyan Arab Jamahiriya evaluated from isotopic data).
Sano, Y., Marty, B., Burnard, P., 2013. Noble gases in the atmosphere. In: The Noble Gases as Geochemical Tracers. Springer, Berlin, Heidelberg, pp. 17–31.
Schmitt, D.N., Lupo, K.D., 2018. On early-Holocene moisture and small-mammal histories in the Bonneville basin, Western United States. The Holocene 28 (3), 492–498. https://doi.org/10.1177/0959683617729453.
Smith, S.P., Kennedy, B.M., 1983. The solubility of noble gases in water and in NaCl brine. Geochim. Cosmochim. Acta 47 (3), 503–515. https://doi.org/10.1016/0016-7037(83)90273-9.
Smith, R.P., Breckenridge, R.P., Wood, T.R., 2011. Preliminary Assessment of Geothermal Resource Potential at the UTTR (No. INL/EXT-11-22215). Idaho National Laboratory (INL).
Solomon, D.K., Cook, P.G., 2000. 3 H and 3 He. In: Environmental Tracers in Subsurface Hydrology. Springer, Boston, MA, pp. 397–424.
Solomon, D.K., Hunt, A., Poreda, R.J., 1996. Source of radiogenic helium 4 in shallow aquifers: Implications for dating young groundwater. Water Resour. Res. 32 (6), 1805–1813. https://doi.org/10.1029/96WR00600.
Stevens, L.E., Meretsky, V.J. (Eds.), 2008. Aridland Springs in North America: Ecology and Conservation. University of Arizona Press.
Stuart, F.M., Lass-Evans, S., Fitton, J.G., Ellam, R.M., 2003. High 3 He/4 He ratios in picritic basalts from Baffin Island and the role of a mixed reservoir in mantle plumes. Nature 424 (6944), 57.
Stute, M., Schlosser, P., 1993. Principles and applications of the noble gas paleothermometer. In: Climate Change in Continental Isotopic Records. vol. 78. pp. 89–100. https://doi.org/10.1029/GM078p0089.
Stuiver, M., Polach, H.A., 1977. Discussion reporting of 14 C data. Radiocarbon 19 (3), 355–363.
Sweetkind, D.S., Cederberg, J.R., Masbruch, M.D., Buto, S.G., 2011. Hydrogeologic framework. In: Heilweil, V.M., Brooks, L.E. (Eds.), 2010. Conceptual Model of the Great Basin Carbonate and Alluvial Aquifer System. US Geological Survey Scientific Investigations Report, vol. 5193. pp. 191.
Tamers, M.A., 1967. Radiocarbon ages of groundwater in an arid zone unconfined aquifer. In: Isotope Techniques in the Hydrologic Cycle. vol. 11. pp. 143–152. https://doi.org/10.1029/GM011p0143.
Tamers, M.A., 1975. Validity of radiocarbon dates on ground water. Geophys. Surv. 2 (2), 217–239.
Tamers, M.A., Scharpenseel, H.W., 1970. Sequential sampling of radiocarbon in groundwater. In: Isotope Hydrology 1970. Proceedings of a Symposium.
Thomas, R.F., Kingsford, R.T., Lu, Y., Cox, S.J., Sims, N.C., Hunter, S.J., 2015. Mapping inundation in the heterogeneous floodplain wetlands of the Macquarie Marshes, using Landsat Thematic Mapper. J. Hydrol. 524, 194–213. https://doi.org/10.1016/j.jhydrol.2015.02.029.
Torgersen, T., Ivey, G.N., 1985. Helium accumulation in groundwater. II: a model for the accumulation of the crustal 4He degassing flux. Geochim. Cosmochim. Acta 49 (11), 2445–2452. https://doi.org/10.1016/0016-7037(85)90244-3.
Toth, J., 1963. A theoretical analysis of groundwater flow in small drainage basins. J. Geophys. Res. 68 (16), 4795–4812. https://doi.org/10.1029/JZ068i016p04795.
Turk, L.J., Davis, S.N., Bingham, C.P., 1973. Hydrogeology of lacustrine sediments, Bonneville Salt Flats, Utah. Econ. Geol. 68 (1), 65–78. https://doi.org/10.2113/gsecongeo.68.1.65.
U.S. Geological Survey, 2019. National Water Information System Data Available on the World Wide Web (USGS Water Data for the Nation). accessed [August 6, 2019], at URL. http://waterdata.usgs.gov/nwis/.
Unmack, P.J., Minckley, W.L., 2008. The Demise of Desert Springs. Aridland Springs in North America: Ecology and Conservation. University of Arizona Press, Tucson, pp. 11–34.
von Rohden, C., Kreuzer, A., Chen, Z., Aeschbach-Hertig, W., 2010. Accumulation of natural SF6 in the sedimentary aquifers of the North China Plain as a restriction on groundwater dating. Isot. Environ. Health Stud. 46 (3), 279–290. https://doi.org/10.1080/10256016.2010.494771.
Waddell, K.M., Seiler, R.L., Santini, M., Solomon, D.K., 1987. Ground-water Conditions in Salt Lake Valley, Utah, 1969–83, and Predicted Effects of Increased Withdrawals From Wells (No. 87). Utah Department of Natural Resources, Division of Water Rights.
Welch, A.H., Bright, D.J., Knochenmus, L.A., 2007. Water resources of the Basin and Range carbonate-rock aquifer system, White Pine County, Nevada, and adjacent areas in Nevada and Utah. US Geol. Surv. Sci. Investig. Rep. 5261, 96.
Whitney, P.E., Hurley, P.M., 1964. The problem of inherited radiogenic strontium in sedimentary age determinations. Geochim. Cosmochim. Acta 28 (4), 425–436. https://doi.org/10.1016/0016-7037(64)90116-4.
Wiersberg, T., Erzinger, J., 2007. A helium isotope cross-section study through the San Andreas Fault at seismogenic depths. Geochem. Geophys. Geosyst. 8 (1). https://doi.org/10.1029/2006GC001388.
Wilde, F.D., Radtke, D.B. (Eds.), 1998. Handbooks for Water-resources Investigations: National Field Manual for the Collection of Water-quality Data. Field Measurements. US Department of the Interior, US Geological Survey.
Winograd, I.J., 1962. Interbasin Movement of Ground Water at the Nevada Test Site. United States Department of the Interior Geological Survey. Water Resources at Digital Scholarship@UNLV. http://digitalscholarship.unlv.edu/water_pubs/124.